A Kinetic Model for Divertors and Pumped Limiters

A.W. Bailey and G.A. Emmert

February 1984
(revised August 1984)

UWFDM-566

Submitted to Nuclear Fusion.

FUSION TECHNOLOGY INSTITUTE

UNIVERSITY OF WISCONSIN

MADISON WISCONSIN

A Kinetic Model for Divertors and Pumped Limiters

A.W. Bailey and G.A. Emmert

Fusion Technology Institute
University of Wisconsin
1500 Engineering Drive
Madison, WI 53706

http://fti.neep.wisc.edu

February 1984 (revised August 1984)

UWFDM-566

Submitted to Nuclear Fusion.

A KINETIC MODEL FOR DIVERTORS AND PUMPED LIMITERS

A.W. Bailey and G.A. Emmert

Fusion Engineering Program
Nuclear Engineering Department
University of Wisconsin-Madison
Madison, Wisconsin 53706

February 1984

UWFDM-566

Submitted to Nuclear Fusion.

A KINETIC MODEL FOR DIVERTORS AND PUMPED LIMITERS

A.W. BAILEY* and G.A. EMMERT

Fusion Engineering Program, Department of Nuclear Engineering
University of Wisconsin-Madison, Madison, WI 53706

ABSTRACT. In divertors and pumped limiters, plasma flows along magnetic field lines from the scrape-off layer to a material wall where it is neutralized. The neutrals refluxing from the wall will undergo ionization and charge exchange, producing cold ions. These cold ions will increase the electric potential over that which would otherwise exist. Depending on the location of their production relative to the peak in the potential, the cold ions will flow down the potential gradient either towards the scrape-off zone or towards the wall. This problem has been examined using a largely analytical, kinetic model. Both the case of a uniform magnetic field and the case of a magnetic field possessing a constriction (as in a bundle divertor) are presented. The effects of charge exchange are included.

*Present address: Nuclear Engineering Department, Georgia Institute of Technology, Atlanta, GA 30332.

1. INTRODUCTION

Plasma flow along magnetic field lines to a neutralizer plate is a common feature of both divertors and limiters in toroidal fusion devices and plasma dumps in linear devices. The plasma striking the plate is neutralized and the resulting gas molecules evolved from the wall interact with the incoming plasma by atomic processes, such as dissociation, charge exchange, and ionization. This produces cold ions which increase the plasma density near the plate. If the electrons are sufficiently collisional to remain close to a Maxwellian distribution, then the electrostatic potential will also increase because of the Boltzmann relationship. Depending on where cold ions are produced (by charge exchange and ionization) relative to the maximum of the potential, the cold ions will be accelerated either towards the plate, or upstream against the incoming hot plasma. The electrostatic potential also reduces the flow of hot plasma to the plate. Consequently, the potential can play a significant role in the recycling processes at the plate.

The above discussion assumes implicitly that the magnetic field is uniform in the recycling zone near the plate. If the field is non-uniform and expanding, as in a bundle divertor, then an additional complication arises. The expansion of the field drops the hot ion density; this competes with the increased ion density created by recycling. Depending on the amount of recycling at the plate, the net effect can be either a positive or negative potential relative to the upstream plasma potential.

A largely analytical, kinetic model for this interaction and recycling process is presented here. The ion motion is assumed to be collisionless (except for atomic processes) over the scale length for ionization and charge exchange. The electrons are assumed to be isothermal and sufficiently close

to a Maxwellian distribution so that the Boltzmann relationship between density, temperature, and potential is satisfied. These assumptions require that the incoming plasma be relatively hot ($\gtrsim$ 100 eV). The magnetic field can be either uniform or have an upstream constriction, as in a bundle divertor. The model calculates the electrostatic potential profile in the quasi-neutral region, and the particle and energy flux of ions, electrons, and neutrals leaving the upstream plasma, entering the sheath and incident on the wall.

The uniform magnetic field version of this problem has also been treated with a large kinetic code by Gierzewski et al. [1], who considered the possible atomic processes in greater detail. Our analysis, which uses a simplified description of the atomic processes, reproduces the significant features of their calculation. For dense, cool plasmas, Coulomb collisional processes become more important and the fluid treatments by Petravic et al. [2] and Seki et al. [3] are more realistic in the collisional regime. The intermediate regime, where the Coulomb mean free paths are comparable to the macroscopic scale lengths, remains unexplored.

This paper is organized as follows. The model for a uniform magnetic field is developed in Section 2 without charge exchange effects. The modifications due to non-uniform magnetic fields, as in bundle divertors, is described in Section 3. Charge exchange between neutrals and ions is incorporated in Section 4. Results for a variety of cases are then presented and discussed in Section 5. In the following we frequently use the term "divertor" for simplicity, but this is also meant to include pumped limiters as well.

2. UNIFORM MAGNETIC FIELD

Consider a plasma flowing along a uniform magnetic field and striking a wall where it is neutralized. The neutral atoms and molecules emitted from the plate re-enter the plasma and are re-ionized. This produces a non-uniform density and potential near the plate, as shown in Fig. 1. It is assumed that there is a single maximum in the potential as shown. This peak separates space into two regions. In region I (see Fig. 1) the electric field accelerates ions towards the plate whereas in region II the electric field accelerates ions away from the plate. The incoming ion distribution function ($v_x < 0$, x large) is chosen to be a Maxwellian on the basis that collisional processes in the upstream plasma have sufficiently randomized the particle velocities. The hot ion distribution function in the recycling zone is then determined by Liouville's theorem. The hot ion density in both region I and II is calculated by integrating the distribution function, f, over velocity space.

In region II the hot ion distribution function is

$$f_H = Ae^{-Mv^2/2T_i} e^{-e\phi/T_i}$$

in the populated region of phase space and zero otherwise. The hot ion density is

$$n_{HII} = 2\pi A \int_{-\infty}^{\sqrt{(2e/M)(\phi_m-\phi(x))}} dv_\parallel \int_0^\infty dv_\perp e^{-Mv_\parallel^2/2T_i} e^{-Mv_\perp^2/2T_i} e^{-e\phi(x)/T_i}$$

or

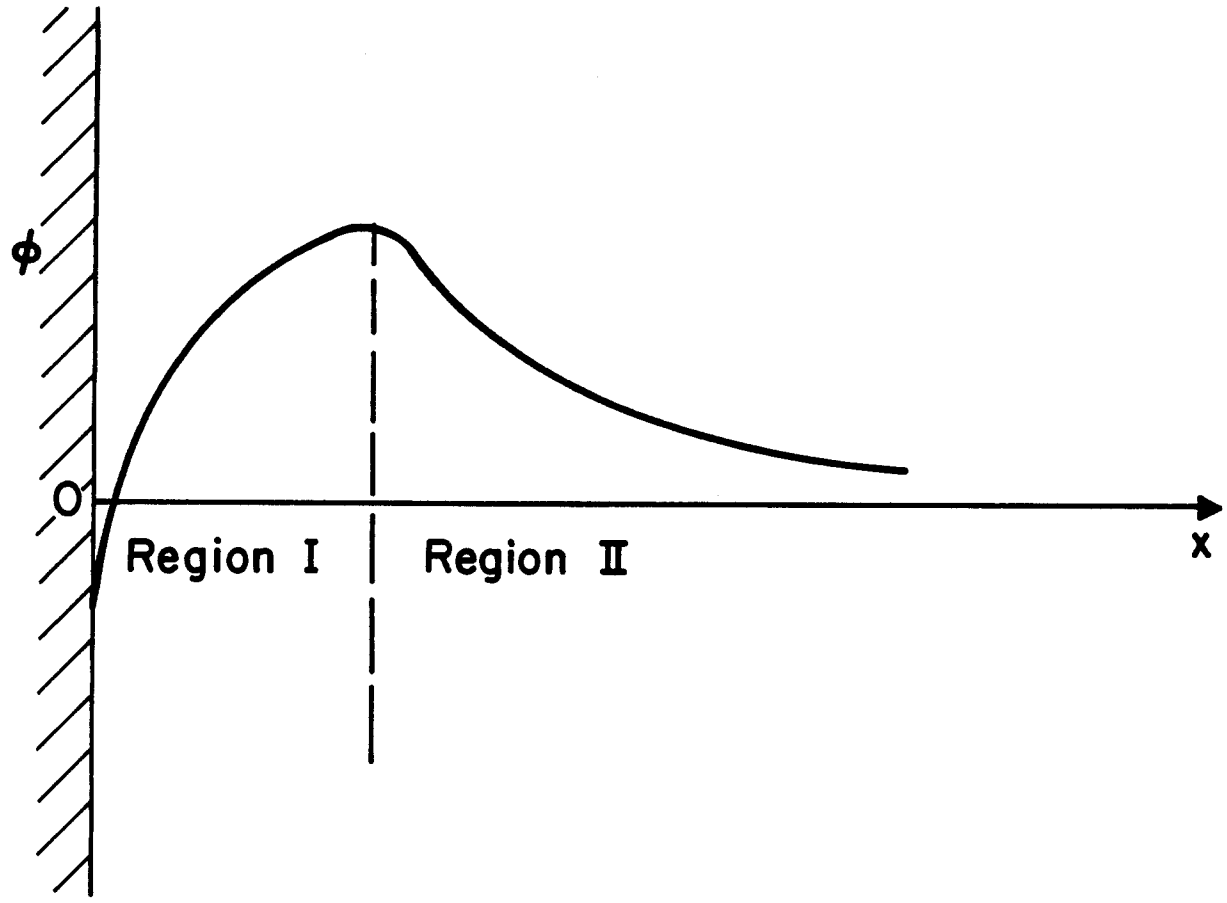

Fig. 1. Conceptual potential profile for hot plasma flowing to a wall in a uniform magnetic field with cold plasma recycling.

$$n_{HII} = 2\pi A e^{-e\phi_t/T_i} \left(\frac{2T_i}{M}\right)^{3/2} \int_0^{\sqrt{\psi_m - \psi(x)}} du_\parallel \, e^{-u_\parallel^2} \int_0^\infty du_\perp \, e^{-u_\perp^2} e^{-\psi(x)} , \quad (1)$$

where A is a normalization constant, M is the ion mass, T_i is the ion temperature in units of energy, $v_\parallel$ and $v_\perp$ are the parallel and perpendicular ion velocities,

$$u_\parallel = \sqrt{\frac{M}{2T_i}} \, v_\parallel ,$$

$$u_\perp = \sqrt{\frac{M}{2T_i}} \, v_\perp ,$$

are the normalized velocities ($u_\parallel > 0$ corresponds to motion away from the plate), $\phi(x)$ is the electric potential at the point x along a field line, ϕ_m is the electric potential at the potential peak, ϕ_t is the potential in the throat of the divertor far enough away from the wall so that essentially all of the neutral gas evolved from the wall has been ionized before reaching that point, and

$$\psi(x) = \frac{e(\phi(x) - \phi_t)}{T_i}$$

$$\psi_m = \frac{e(\phi_m - \phi_t)}{T_i}$$

are normalized potentials. The upper velocity limit is set by requiring that f = 0 for ions with velocities high enough to overcome the potential hill (see Fig. 1), that is, where

$$u_\parallel^2 + \psi > \psi_m \quad (2)$$

and $u_{\parallel} > 0$. These ions would have been emitted by the plate. The plate is assumed to emit only neutral particles in this analysis. Performing the integration in Eq. (1) gives

$$n_{HII} = A' e^{-\psi} [1 + \mathrm{erf}(\sqrt{\psi_m - \psi})] \tag{3}$$

where

$$\mathrm{erf}(x) = \frac{2}{\sqrt{\pi}} \int_0^x dt\, e^{-t^2}$$

is the error function and

$$A' = \frac{A}{2} \left(\frac{2\pi T_i}{M}\right)^{3/2} e^{-e\phi_t/T_i} \,. \tag{4}$$

It can be seen that A' is the density of downstream-going hot ions in the divertor throat. In region I downstream of the peak in the potential, the hot ion density will be

$$n_{HI} = 2\pi A \int_{-\infty}^{-\sqrt{(2e/M)(\phi_m - \phi)}} dv_{\parallel} \int_0^{\infty} dv_{\perp}\, v_{\perp} e^{-Mv_{\parallel}^2/2T_i} e^{-Mv_{\perp}^2/2T_i} e^{-e\phi/T_i}$$

which becomes

$$n_{HI} = A' e^{-\psi} [1 - \mathrm{erf}(\sqrt{\psi_m - \psi})] \,. \tag{5}$$

Let Γ_w be the flux of hot ions striking the wall. If a fraction f_p of the resulting neutrals are pumped away, a fraction $(1 - f_p)$ will reappear as cold ions upon re-ionization. If f_x is the fraction of those reappearing ions which are ionized upstream of the point at which the potential peaks, a fraction $(1 - f_x)$ will return to the wall. Those cold ions striking the wall will also reflux as neutrals and a fraction of them will themselves become

cold ions which will strike the wall. The total flux of hot and cold ions to the wall will thus be

$$\frac{\Gamma_w}{1 - (1 - f_p)(1 - f_x)} .$$

If the plasma flowing to the divertor is hot, then ions produced by ionization of neutral gas evolved from the wall will be born with energies that are small compared to the hot ion velocity, and so their thermal motion can be ignored. A cold ion can then be considered to have a velocity at a point such that its kinetic energy is equal to the difference between the potential at that point and the potential at which it was created. The cold ion density will be given by

$$n_c(x) = \sqrt{\frac{M}{2e}} \left| \int_{x_o}^{x} dx' \frac{S(x')}{\sqrt{\phi(x') - \phi(x)}} \right| . \qquad (6)$$

The ionization source function S(x) can be written as

$$S(x) = S_o h(\psi(x)) \frac{d\psi}{dx} \qquad (7)$$

with h(x) normalized such that

$$\int h(\psi(x))\, d\psi = 1 .$$

Thus S_o is the total number of cold ions created per unit wall area, and h(x) carries the information about the spatial profile of S(x). Letting

$$S_o = \frac{(1 - f_p)}{1 - (1 - f_p)(1 - f_w)} \Gamma_w \tag{8}$$

the cold ion density can be written as

$$n_C = \Gamma_w \frac{(1 - f_p)}{1 - (1 - f_p)(1 - f_x)} \sqrt{\frac{M}{2T_i}} \int_{\psi}^{\psi_m} \frac{h(\psi')}{\sqrt{\psi' - \psi}} . \tag{9}$$

The flux of hot ions to the wall will be

$$\Gamma_w = -2\pi A \exp\left(-\frac{e\phi_m}{T_i}\right) \int_{-\infty}^{o} dv_{\parallel} \, v_{\parallel} \exp\left(-\frac{Mv_{\parallel}^2}{2T_i}\right) \int_{o}^{\infty} dv_{\perp} \, v_{\perp} \exp\left(-\frac{Mv_{\perp}^2}{2T_i}\right)$$

$$= A' \sqrt{\frac{2T_i}{\pi M}} \, e^{-\psi_m} . \tag{10}$$

The cold ion density becomes

$$n_C = \frac{A'}{\sqrt{\pi}} P e^{-\psi_m} \int_{\psi_m}^{\psi} d\psi' \frac{h(\psi')}{\sqrt{\psi' - \psi}} , \tag{11}$$

where

$$P = \frac{(1 - f_p)}{1 - (1 - f_p)(1 - f_x)} .$$

The electrons are assumed to have a Boltzmann distribution

$$n_e = \lambda A' e^{\tau\psi} , \tag{12}$$

where

$$\tau = \frac{T_i}{T_e} ,$$

T_e is the electron temperature and λ is the ratio in the divertor throat of the total ion density to the downstream-going hot ion density where the down-

stream-going region of velocity space is filled (as it is in this case). A large value of λ thus implies a high density of cold ions and a small value of λ implies a low density of cold ions.

The electric fields in the divertor will be weak except very near the wall due to the fact that the mean free path for neutral ionization will be large compared to the Debye length; thus, the plasma can be assumed to be quasi-neutral outside the sheath. For a hydrogenic plasma

$$n_C = n_e - n_H \ . \tag{13}$$

So in region I

$$\frac{Pe^{-\psi_m}}{\sqrt{\pi}} \int_{\psi}^{\psi_m} d\psi' \ \frac{h(\psi')}{\sqrt{\psi' - \psi}} = \lambda e^{\tau\psi} - e^{-\psi}\left[1 - \mathrm{erf}\left(\sqrt{\psi_m - \psi}\right)\right] \ , \tag{14}$$

and in region II

$$\frac{Pe^{-\psi_m}}{\sqrt{\pi}} \int_{\psi}^{\psi_m} d\psi' \ \frac{h(\psi')}{\sqrt{\psi' - \psi}} - \lambda e^{\tau\psi} - e^{-\psi}\left[1 + \mathrm{erf}\left(\sqrt{\psi_m - \psi}\right)\right] \ . \tag{15}$$

Let

$$\eta = \psi_m - \psi \ ,$$

then, assuming η varies monotonically with x in each region,

$$\frac{Pe^{-\psi_m}}{\sqrt{\pi}} \int_{0}^{\eta} d\eta' \ \frac{h(\eta')}{\sqrt{\eta - \eta'}} = \lambda e^{\tau\psi_m} e^{-\tau\eta} - e^{-\psi_m} e^{\eta}\left[1 \pm \mathrm{erf}\left(\sqrt{\eta}\right)\right] \ , \tag{16}$$

where the (-) is used in region I and the (+) is used in region II. Equation (16) is the integral equation determining η. An Abel inversion [4] gives

$$\frac{Pe^{-\psi_m}}{\sqrt{\pi}}\, h(\eta) = \frac{1}{\pi}\frac{d}{d\eta}\int_0^{\eta} d\eta' \, \frac{\lambda e^{\tau\psi_m} e^{-\tau\eta'} - e^{\psi_m} e^{\eta'}\left[1 \pm \mathrm{erf}(\sqrt{\eta'})\right]}{\sqrt{\eta - \eta'}} .$$

Evaluating the integral gives the results

$$\frac{Pe^{-\psi_m}}{\sqrt{\pi}}\, h(\eta) = \frac{1}{\pi}\frac{d}{d\eta}\left[\frac{2\lambda}{\sqrt{\tau}} e^{\tau\psi_m} e^{-\tau\eta} D(\sqrt{\tau\eta}) - \sqrt{\pi}\, e^{-\psi_m} e^{\eta} \mathrm{erf}(\sqrt{\eta}) \mp \sqrt{\pi}\, e^{-\psi_m}(e^{\eta} - 1)\right] , \tag{17}$$

where $$D(x) = \int_0^x dt\, e^{-t^2}$$

is Dawson's integral [5]. Integrating the cold ion source profile, h, from the potential peak to the throat yields f_x, the fraction of the neutrals ionized upstream of the potential peak, so

$$Pe^{-\psi_m} f_x = \frac{2\lambda}{\sqrt{\pi\tau}} D(\tau\psi_m) - \mathrm{erf}(\sqrt{\psi_m}) - 1 + e^{-\psi_m} . \tag{18}$$

Integrating from the peak to the sheath edge gives

$$Pe^{-\psi_m}(1-f_x) = \frac{2\lambda}{\sqrt{\pi\tau}} D(\sqrt{\tau(\psi_m - \psi_s)})\, e^{\tau\psi_s} - e^{-\psi_s}\mathrm{erf}(\sqrt{\psi_m - \psi_s}) + e^{-\psi_s} - e^{-\psi_m} \tag{19}$$

where $$\psi_s = \frac{e(\phi_s - \phi_t)}{T_i}$$

and ϕ_s is the potential at the sheath edge. Equation (18) is a transcendental equation for ψ_m, given f_x and λ. After solving Eq. (18) for ψ_m, Eq. (19) can be solved for ψ_s. Only certain values of f_x and λ will give solutions that

are monotonic in each region, i.e. decreasing as one moves away from the potential peak. These limits can be determined by performing the integration indicated in Eq. (26), giving

$$\frac{Pe^{-\psi_m}}{\sqrt{\pi}}\, h(\eta) = \frac{1}{\pi}\left\{\lambda e^{\tau\psi_m}\left[\frac{1}{\sqrt{\eta}} - 2\sqrt{\tau}\, e^{-\tau\eta}\, D\left(\sqrt{\tau\eta}\right)\right] - \sqrt{\pi}\, e^{-\psi_m}\, e^{\eta}\, \mathrm{erf}\left(\sqrt{\eta}\right)\right.$$
$$\left. - \frac{e^{-\psi_m}}{\sqrt{\eta}} \mp \sqrt{\pi}\, e^{-\psi_m}\, e^{\eta}\right\} . \tag{20}$$

Now $h(\eta)$ must be non-negative everywhere. Ionization creates cold ions; it does not destroy them. Enforcing the requirement that $h(\eta) \geq 0$ at the divertor throat ($\eta = \psi_m$) in region II gives the inequality

$$\lambda \geq \left[\mathrm{erf}\left(\sqrt{\psi_m}\right) + \frac{e^{-\psi_m}}{\sqrt{\pi\psi_m}} + 1\right]\left\{\frac{e^{\tau\psi_m}}{\sqrt{\pi}}\left[\frac{1}{\sqrt{\psi_m}} - 2\sqrt{\tau}\, e^{-\tau\psi_m}\, D\left(\sqrt{\tau\psi_m}\right)\right]\right\}^{-1} \tag{21}$$

and enforcing the requirement that $h(\eta) \geq 0$ at the sheath edge ($\eta = \psi_m - \psi_s$) in region I gives

$$\lambda \geq \left[e^{-\psi_s}\, \mathrm{erf}\left(\sqrt{\psi_m - \psi_s}\right) + \frac{e^{-\psi_m}}{\sqrt{\pi(\psi_m - \psi_s)}} - e^{-\psi_s}\right]\left\{\frac{e^{\tau\psi_m}}{\sqrt{\pi}}\left[\frac{1}{\sqrt{\psi_m - \psi_s}}\right.\right.$$
$$\left.\left. - 2\sqrt{\tau}\, e^{-\tau(\psi_m - \psi_s)}\, D\left(\sqrt{\tau(\psi_m - \psi_s)}\right)\right]\right\}^{-1} . \tag{22}$$

Choosing equality in Eqs. (21) and (22) generally maximizes the energy flow to the divertor. These two equations fix the value of both f_x and λ. The energy flux is generally maximized in this case due to the fact that the potential gradient is the steepest and so the cold ions in region I enter the sheath with the greatest velocity. Also a low value of λ decreases the po-

tential rise between the scrape-off layer and the divertor throat, as will shortly be discussed, and so maximizes the particle flux into the divertor. That the lowest value for λ always gives the maximum energy flow has not been proven; it is only an empirical observation. It is likely that the state which maximizes the energy flux to the wall will be the one that is physically realized, but it is also possible that some other condition will determine the values of f_x and λ.

Given a value of λ, it is possible to compute the potential in the divertor chamber relative to the potential in the divertor throat. The potential in the divertor throat will, however, generally not be the same as the potential in the scrape-off layer. There will be a transition region of a mean free path thickness between the scrape-off layer where the distribution function is Maxwellian and the throat where the distribution function is largely forward-going. Over this transition region, the density and potential can vary. A precise calculation of the potential difference between the scrape-off layer and the divertor throat is beyond the scope of this paper and would require a spatially dependent Fokker-Planck analysis. However, a simple estimate can be easily obtained by assuming that the downstream-going hot ions flow collisionlessly from a Maxwellian distribution in the scrape-off layer to the throat. The ratio of the ion density in the throat, n_{Ht}, to the ion density in the scrape-off layer, n_{Hs}, will then be

$$\frac{n_{Ht}}{n_{Hs}} = \frac{\lambda}{2} e^{\psi_c} , \tag{23}$$

where

$$\psi_c = \frac{e(\phi_c - \phi_t)}{T_i}$$

and ϕ_c is the potential in the scrape-off layer. For Boltzmann electrons the ratio of the electron densities will be

$$\frac{n_{et}}{n_{es}} = e^{-\tau\psi_c} . \tag{24}$$

These ratios must be the same, so

$$\frac{\lambda}{2} e^{\psi_c} = e^{-\tau\psi_c} ,$$

or

$$\psi_c = - \frac{\ln\left(\frac{\lambda}{2}\right)}{\tau + 1} . \tag{25}$$

For the case of no pumping with $\lambda = \lambda_{min} = 2.63$ and $\tau = 1$, $\psi_c = -0.137$. For larger values of λ, the magnitude of ψ_c will be larger.

If the pumping is strong enough, it is possible to have a potential which drops monotonically from the scrape-off layer to the wall. This is a limiting case of the previous treatment for region I, i.e. with $f_x = 0$ and $\psi_m = 0$. In this case the equation for quasi-neutrality (29) reduces to

$$P = \frac{2}{\sqrt{\pi\tau}} D\left(\sqrt{-\tau\psi_s}\right) e^{\tau\psi_s} - e^{-\psi_s} \operatorname{erf}\left(\sqrt{-\psi_s}\right) + e^{-\psi_s} - 1 . \tag{26}$$

Here the requirement on λ for a monotonic potential profile within the divertor reduces to

$$\lambda \geq \left[e^{-\psi_s} \operatorname{erf}\left(\sqrt{-\psi_s}\right) + \frac{1}{\sqrt{-\pi\psi_s}} - e^{-\psi_s}\right]\left\{\frac{1}{\sqrt{\pi}}\left[\frac{1}{\sqrt{-\psi_s}} - 2\sqrt{\tau}\, e^{\tau\psi_s} D\left(\sqrt{-\tau\psi_s}\right)\right]\right\}^{-1} . \tag{27}$$

As before, the maximum energy flux will generally exist for the smallest value

of λ which gives a monotonic profile. Purely falling solutions can only exist for $\lambda \leq 2$, since otherwise the potential would be higher in the divertor throat than in the scrape-off layer. For $T_e = T_i$, monotonically falling solutions are only possible where $f_p \geq 0.60$. Even for $\lambda \leq 2$ there can be a non-negligible cold ion density in the throat; but these ions will be traveling very slowly, so the cold ion flux to the scrape-off layer will be negligible. The cold ions are recycled by the potential back to the neutralizer plate.

The other limiting case, that in which the potential peaks at the sheath edge, has been discussed in a previous paper [6]. This case is always found to give a smaller energy flow than the case in which the potential peaks away from the wall, and thus is not expected to occur. Before presenting results for a uniform field, we consider the extension of this model to bundle divertors and then include charge exchange effects. Various results for typical cases will be presented in Section 5.

3. BUNDLE DIVERTORS

Bundle divertors have an additional complication compared to poloidal divertors and pumped limiters in that they possess a magnetic constriction in the divertor throat. This can be modeled by dividing the plasma into three regions: the scrape-off layer, the divertor throat, and the divertor chamber, each with its own value of the magnetic field strength (see Figs. 2 and 3). All of the reionization of neutrals from the wall will be assumed to occur in the divertor chamber. Jumps in the electric potential can occur at the steps in the magnetic field. In an actual device, of course, changes in the magnetic field and electric potential would be smooth.

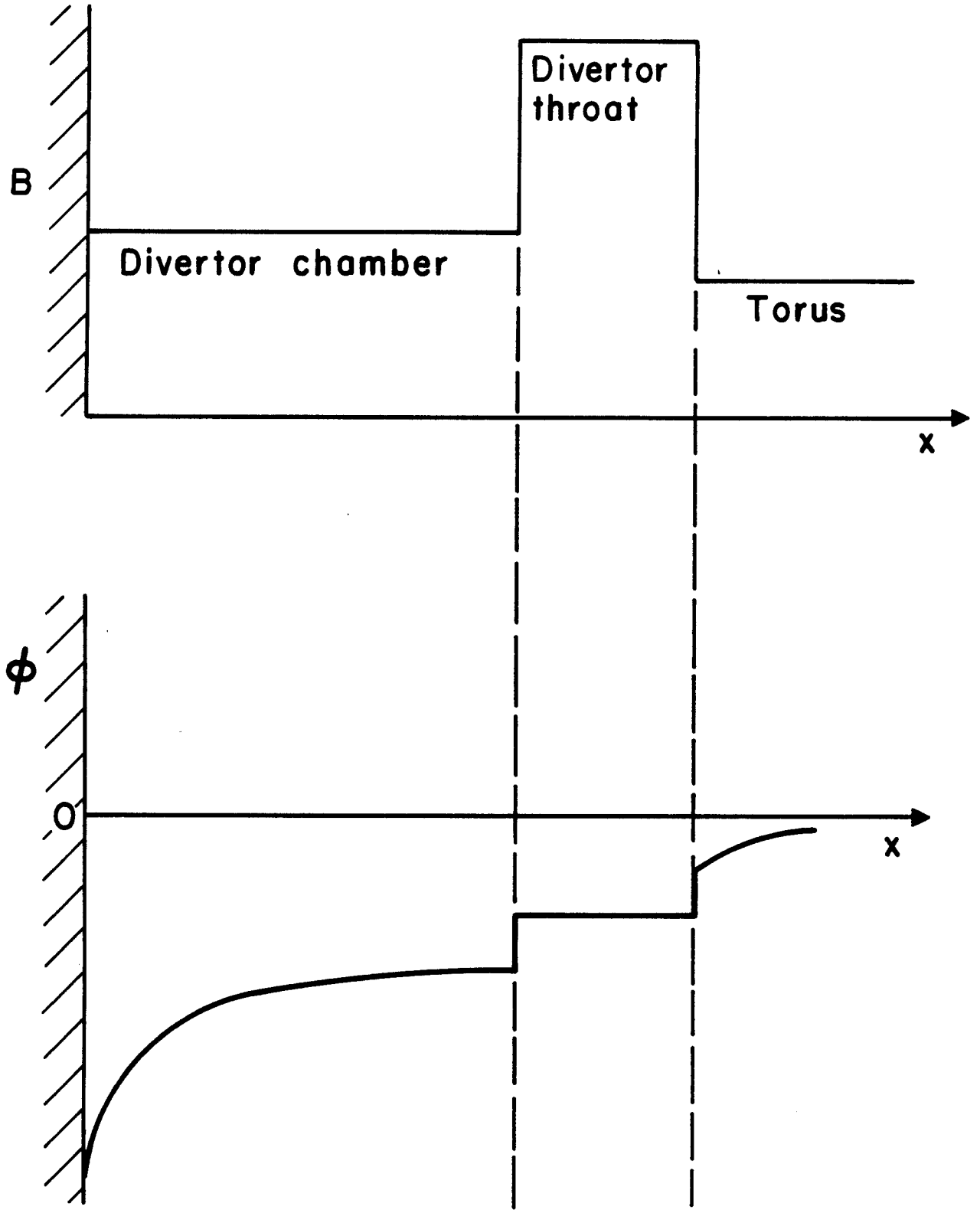

Fig. 2. Conceptual model for the magnetic fields and electric potential profile in a strongly pumped bundle divertor. The jumps in the magnetic field cause jumps in the electric potential.

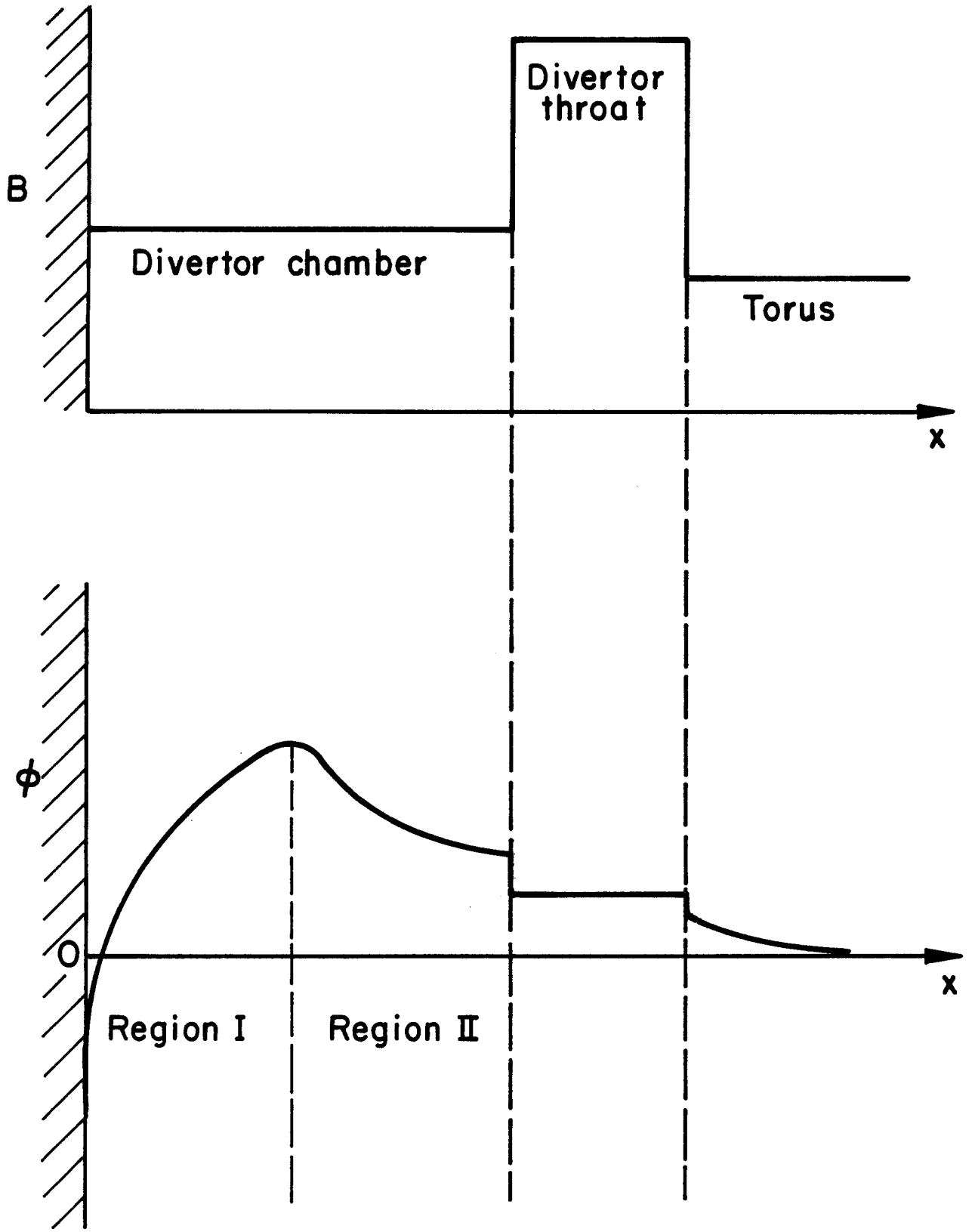

Fig. 3. Conceptual model for the magnetic fields and electric potential profile in a weakly pumped bundle divertor. The jumps in the magnetic field cause jumps in the electric potential.

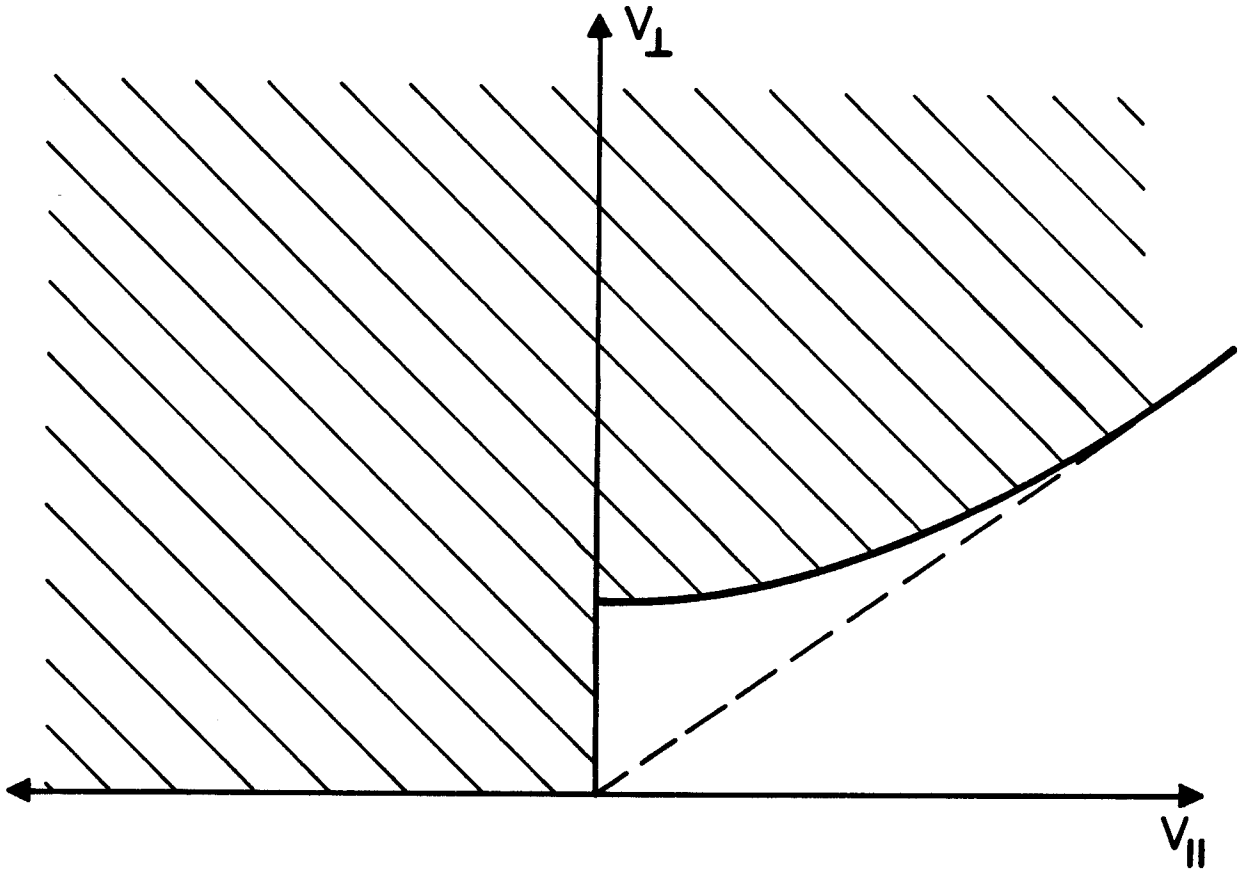

Fig. 4. The hatching shows the populated region of velocity space for hot ions just upstream of the magnetic constriction in a bundle divertor with an electric potential that falls monotonically from the scrape-off layer to the divertor target. A portion of the downstream-going ions ($v_{||} < 0$) will mirror; the rest will flow to the divertor throat.

First consider the case of a potential that is purely falling from the scrape-off layer to the divertor plate, as shown in Fig. 2. The case in which there is no neutral reflux has previously been treated by Emmert [7]. A similar treatment with neutral recycling is possible. Consider ions flowing through the divertor. Just upstream of the magnetic field constriction the ion velocity space will be as shown in Fig. 4. Hot ions will flow downstream into the divertor but a fraction of them will mirror off of the increase in the magnetic field strength. There will be an empty region of velocity space since there will be no upstream-going particles corresponding to the downstream-going particles which are able to pass through the divertor throat. On the boundary between the empty and filled regions of velocity space,

$$u_{\parallel u}^2 + u_{\perp u}^2 + \psi_u = u_{\parallel t}^2 + u_{\perp t}^2 ,$$

$$u_{\perp t}^2 = R_u u_{\perp u}^2 ,$$

where the "t" and "u" subscripts refer to the values in the divertor throat and to the values just upstream of the magnetic constriction, respectively. Here R_u is the upstream mirror ratio, i.e. $B_{throat}/B_{scrape\text{-}off}$; and

$$\psi_u = \frac{e(\phi_u - \phi_t)}{T_i} .$$

So for the reflected ions

$$u_{\perp u}^2 > \frac{u_{\parallel u}^2 + \psi_u}{R_u - 1} . \qquad (28)$$

If the ion distribution function in the hatched region of velocity space shown in Fig. 4 is taken to be locally Maxwellian, the ion density at the upstream

point will be

$$n_{Hu} = 2\pi A \left(\frac{2T_i}{M}\right)^{3/2} e^{-e\phi_u/T_i} \int_{-\infty}^{o} du_{\parallel}\, e^{-u_{\parallel}^2} \int_{o}^{\infty} du_{\perp}\, u_{\perp} e^{-u_{\perp}^2}$$

$$+ 2\pi A \left(\frac{2T_i}{M}\right)^{3/2} e^{-e\phi_u/T_i} \int_{o}^{\infty} du_{\parallel}\, e^{-u_{\parallel}^2} \int_{\sqrt{(u_{\parallel}^2+\psi_u)/(R_u-1)}}^{\infty} du_{\perp}\, u_{\perp} e^{-u_{\perp}^2}$$

where the first term represents the downstream-going ions and the second term the ions that reflect off of the stronger magnetic field in the divertor throat. Performing the integrations gives

$$n_{Hu} = A'\left(e^{-\psi_u} + \frac{e^{-\gamma_u \psi_u}}{\sqrt{\gamma_u}}\right) \tag{29}$$

where

$$\gamma_u = \frac{R_u}{R_u - 1} . \tag{30}$$

In the divertor throat, the hot ion velocity space will be as shown in Fig. 5. Only downstream-going ions will be present. There will be an additional empty region of velocity space due to the potential drop, ψ_u, between the upstream point and the divertor throat. The boundary between the filled and unfilled regions of velocity space will be set by the conditions that

$$u_{\perp t}^2 > \gamma_u (\psi_u - u_{\parallel t}^2) \tag{31}$$

so the density in the throat will be

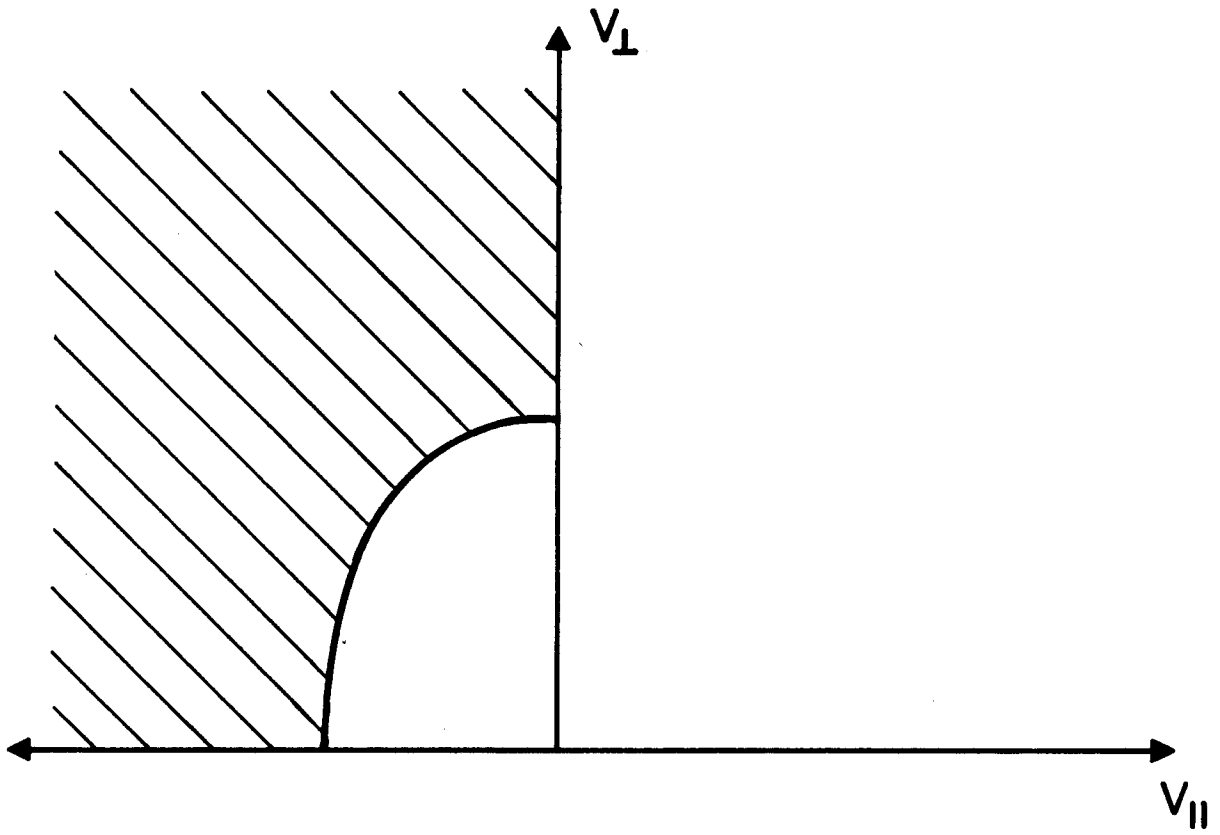

Fig. 5. The hatching shows the populated region with an electric potential that falls monotonically from the scrape-off layer to the divertor target. The potential drop, ψ_u, produces an empty region in the downstream-going velocity space ($v_{||} < 0$).

$$n_{Ht} = 2\pi A \left(\frac{2T_i}{M}\right)^{3/2} e^{-e\phi_u/T_i} \left[\int_{\sqrt{\psi_u}}^{o} du_\parallel e^{-u_\parallel^2} \int_{\sqrt{\gamma_u(\psi_u - u_\parallel^2)}}^{\infty} du_\perp u_\perp e^{-u_\perp^2}\right.$$

$$\left. + \int_{-\infty}^{-\sqrt{\psi_u}} du_\parallel e^{-u_\parallel^2} \int_{o}^{\infty} du_\perp u_\perp e^{-u_\perp^2}\right] \qquad (32)$$

$$= A'\left[2\sqrt{\frac{R_u - 1}{\pi}} e^{-\gamma_u\psi_u} D\left(\sqrt{\frac{\psi_u}{R_u - 1}}\right) + 1 - \mathrm{erf}\left(\sqrt{\psi_u}\right)\right] .$$

Quasi-neutrality in the divertor throat implies that

$$\lambda = 2\sqrt{\frac{R_u - 1}{\pi}} e^{-\gamma_u\psi_u} D\left(\sqrt{\frac{\psi_u}{R_u - 1}}\right) + 1 - \mathrm{erf}\left(\sqrt{\psi_u}\right) , \qquad (33)$$

where λ, as before, is the normalized electron density in the divertor throat. Quasi-neutrality at the upstream point implies

$$\lambda e^{\tau\psi_u} = e^{-\psi_u} + \frac{e^{-\gamma_u\psi_u}}{\sqrt{\gamma_u}} . \qquad (34)$$

λ can be eliminated to give an equation for ψ_u:

$$\left(e^{-\psi_u} + \frac{e^{-\gamma_u\psi_u}}{\sqrt{\gamma_u}}\right) e^{-\tau\psi_u} = 2\sqrt{\frac{R_u - 1}{\pi}} e^{-\gamma_u\psi_u} D\left(\sqrt{\frac{\psi_u}{R_u - 1}}\right) + 1 - \mathrm{erf}\left(\sqrt{\psi_u}\right) . \qquad (35)$$

With this equation it is possible to solve for the value of ψ_u. λ can then be found using either Eq. (33) or (34).

By conservation of energy,

$$u_{\parallel t}^2 + u_{\perp t}^2 = u_{\parallel}^2 + u_{\perp}^2 + \psi \ , \tag{36}$$

where the right hand side refers to the values in the divertor chamber. Now

$$R_d u_{\perp}^2 = u_{\perp t}^2 \tag{37}$$

where R_d is the downstream mirror ratio, $B_{throat}/B_{divertor\ chamber}$. In the divertor throat there is the requirement that

$$u_{\parallel t}^2 \geq \psi_u - \frac{u_{\perp t}^2}{\gamma_u} \ ,$$

from Eq. (31). Using Eqs. (30), (31), and (37), this requirement becomes

$$\psi_u + \frac{R_d}{R_u} u_{\perp}^2 \leq u_{\parallel}^2 + u_{\perp}^2 + \psi \ . \tag{38}$$

From Eqs. (36) and (37) there is also the requirement that

$$R_d u_{\perp}^2 \leq u_{\parallel}^2 + u_{\perp}^2 + \psi \ . \tag{39}$$

These two conditions determine the populated region of velocity space. If $R_d < R_u$ (see Fig. 6), the hot ion density will be

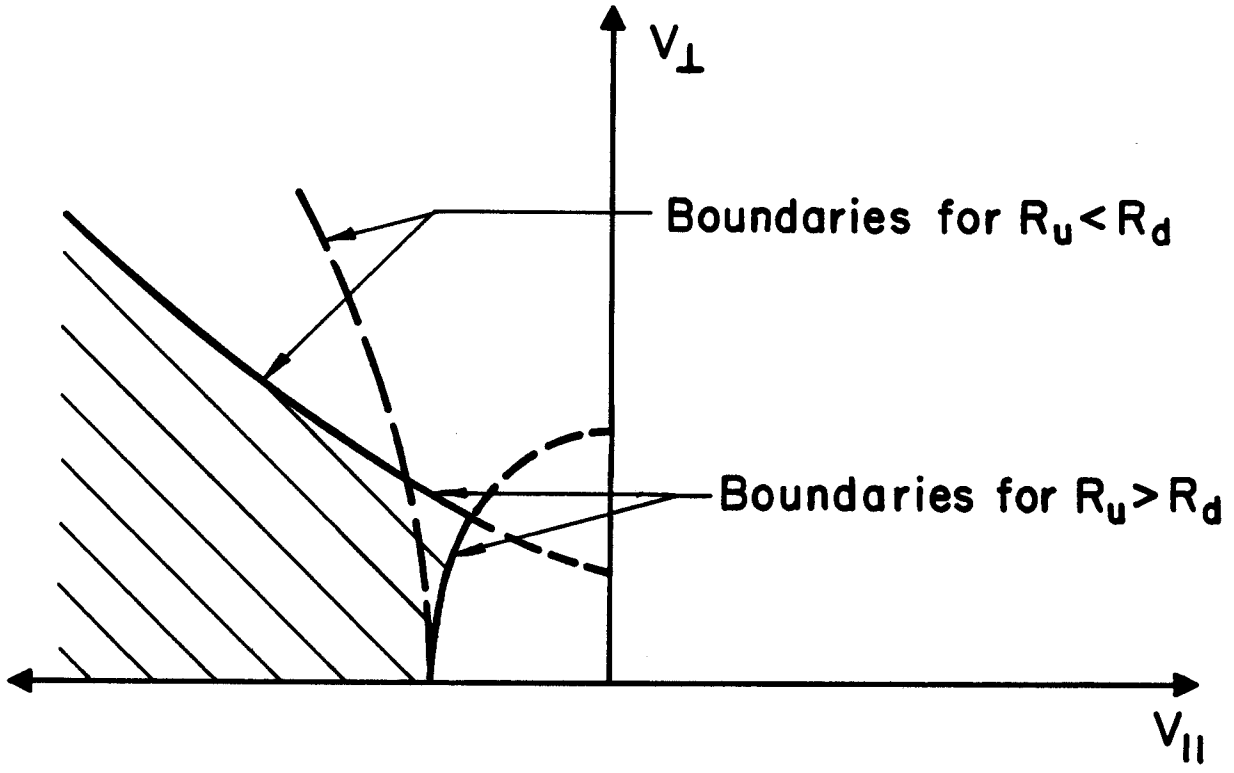

Fig. 6. The hatching shows the populated region of velocity space for hot ions in the divertor chamber of a bundle divertor with an electric potential that falls monotonically from the scrape-off layer to the divertor target.

$$n_H = 2\pi A \left(\frac{2T_i}{M}\right)^{3/2} e^{-e\phi/T_i} \left[\int_{-\sqrt{\psi_u-\psi}}^{-\sqrt{(\gamma_u/\gamma_d)\psi_u-\psi}} du_\parallel\, e^{-u_\parallel^2} \int_{\sqrt{\gamma_h(\psi_u-\psi-u_\parallel^2)}}^{\sqrt{(u_\parallel^2+\psi)/(R_d-1)}} du_\perp\, u_\perp e^{-u_\perp^2}\right.$$

$$\left. + \int_{-\infty}^{-\sqrt{\psi_u-\psi}} du_\parallel\, e^{-u_\parallel^2} \int_{0}^{\sqrt{(u_\parallel^2+\psi)/(R_d-1)}} du_\perp\, u_\perp e^{-u_\perp^2}\right]$$

$$= A'\left\{e^{-\psi}\left[1 - \mathrm{erf}\left(\sqrt{\psi_u - \psi}\right)\right] - \frac{e^{-\gamma_d\psi}}{\sqrt{\gamma_d}}\left[1 - \mathrm{erf}\left(\sqrt{\gamma_u\psi_u - \psi_d\psi}\right)\right] + e^{-\gamma_h\psi_u} e^{(\gamma_h-1)\psi}\right.$$

$$\left. \times \frac{2}{\sqrt{(\gamma_h - 1)\pi}}\left[D\left(\sqrt{(\gamma_h - 1)(\psi_u - \psi)}\right) - D\left(\sqrt{(\gamma_h - 1)\left[(\gamma_u/\gamma_d)\psi_u - \psi\right]}\right)\right]\right\}, \quad (40)$$

where

$$\gamma_d = \frac{R_d}{R_d - 1} \quad (41)$$

and

$$\gamma_h = \frac{R_u}{R_u - R_d}\,. \quad (42)$$

If $R_d > R_u$ (see Fig. 6), the hot ion density will be

$$n_H = 2\pi A e^{-e\phi/T_i} \left(\frac{2T_i}{M}\right)^{3/2} \left[\int_{-\sqrt{(\gamma_u/\gamma_d)\psi_u - \psi}}^{-\sqrt{\psi_u - \psi}} du_\parallel \, e^{-u_\parallel^2} \int_0^{\sqrt{|\gamma_h|(u_\parallel^2 + \psi - \psi_u)}} du_\perp \, u_\perp e^{-u_\perp^2}\right.$$

$$\left. + \int_{-\infty}^{-\sqrt{(\gamma_u/\gamma_d)\psi_u - \psi}} du_\parallel \, e^{-u_\parallel^2} \int_0^{\sqrt{(u_\parallel^2 + \psi)/(R_d - 1)}} du_\perp \, u_\perp e^{-u_\perp^2}\right]$$

$$= A' \left\{ e^{-\psi} \left[1 - \mathrm{erf}\left(\sqrt{\psi_u - \psi}\right)\right] - \frac{e^{-\gamma_d \psi}}{\sqrt{\gamma_d}} \left[1 - \mathrm{erf}\left(\sqrt{\gamma_u \psi_u - \gamma_d \psi}\right)\right] - \frac{e^{-\gamma_h \psi_u} e^{(\gamma_h - 1)\psi}}{\sqrt{1 - \gamma_h}} \right.$$

$$\left. \times \left[\mathrm{erf}\left(\sqrt{(1 - \gamma_h)\left((\gamma_u/\gamma_d)\psi_u - \psi\right)}\right) - \mathrm{erf}\left(\sqrt{(1 - \gamma_h)(\psi_u - \psi)}\right)\right]\right\} . \qquad (43)$$

The hot ion flux to the wall will then be

$$\Gamma_w = -\frac{2\pi A}{R_d} \left(\frac{2T_i}{M}\right)^2 e^{-e\phi_t/T_i} \left[\int_{-\sqrt{\psi_u}}^{0} du_\parallel \, u_\parallel e^{-u_\parallel^2} \int_{\sqrt{\gamma_u(\psi_u - u_\parallel^2)}}^{\infty} du_\perp \, u_\perp e^{-u_\perp^2}\right.$$

$$\left. + \int_{-\infty}^{-\sqrt{\psi_u}} du_\parallel \, u_\parallel e^{-u_\parallel^2} \int_0^{\infty} du_\perp \, u_\perp e^{-u_\perp^2}\right]$$

$$= \frac{A'}{R_d} \sqrt{\frac{2T_i}{\pi M}} \left(\frac{e^{(\gamma_u - 1)\psi_u} - 1}{\gamma_u - 1} e^{-\gamma_u \psi_u} + e^{-\psi_u}\right) . \qquad (44)$$

Equation (13) then becomes

$$\Gamma_w P \sqrt{\frac{M}{2T_i}} \int_0^{\eta} d\eta' \frac{h(\eta')}{\sqrt{\eta - \eta'}} = n_e(\eta) - n_H(\eta) \ , \tag{45}$$

where $\eta = \psi_m - \psi$ as before. The maximum energy flow occurs for the case in which $\psi_m = 0$, so that there is no change in the potential at the transition between the divertor throat and the divertor chamber. Abel inverting Eq. (45) and evaluating the expression at the sheath edge ($\eta = -\psi_s$) gives

$$\Gamma_w P \sqrt{\frac{M}{2T_i}} = \frac{1}{\pi} \int_0^{-\psi_s} d\eta' \frac{n_e(\eta') - n_H(\eta')}{\sqrt{-\psi_s - \eta'}} \ . \tag{46}$$

In this case there is no solution for the integral in terms of familiar functions. Either the integral must be computed numerically or approximations must be made for the integrand.

If the pumping is decreased, λ will rise as cold ions flow into the divertor throat. Above a certain point a sufficient number of cold ions will be present to raise the potential in the throat high enough to allow cold ions to flow to the scrape-off layer. In this case a peaked potential profile will form in the divertor, as shown in Fig. 3. Cold ions produced upstream of the potential peak (region II) will flow out of the divertor, while cold ions produced downstream of the peak (region I) will flow to the wall. In order to determine the potential in region II, it is necessary to solve simultaneously an equation for quasi-neutrality in the divertor chamber and an equation of quasi-neutrality in the divertor throat.

Next we consider region II of the divertor chamber. In addition to the downstream-going ions, there will also be ions that have reflected off of the peak in the electric potential. The hot ion density will thus be

$$n_H = 2\pi A \left(\frac{2T_i}{M}\right)^{3/2} e^{-e\phi/T_i} \int_{-\infty}^{\sqrt{\psi_m-\psi}} du_\parallel\, e^{-u_\parallel^2} \int_0^{\sqrt{(u_\parallel^2+\psi)/(R_d-1)}} du_\perp\, u_\perp e^{-u_\perp^2}$$

$$= A'\{e^{-\psi}[1 + \mathrm{erf}(\sqrt{\psi_m - \psi})] - \frac{e^{-\gamma_d\psi}}{\sqrt{\gamma_d}}\,[1 + \mathrm{erf}(\sqrt{\gamma_d(\psi_m - \psi)})]\} \,. \qquad (47)$$

The hot ion flux to the wall will be

$$\Gamma_w = -2\pi A e^{-\psi_m} \left(\frac{2T_i}{M}\right)^{3/2} \int_{-\infty}^{0} du_\parallel\, u_\parallel e^{-u_\parallel^2} \int_0^{\sqrt{(u_\parallel+\psi)/(R_d-1)}} du_\perp\, u_\perp e^{-u_\perp^2}$$

$$= A' \sqrt{\frac{2T_i}{\pi M}} \left(e^{-\psi_m} - \frac{e^{-\gamma_d\psi_m}}{\gamma_d}\right) .$$

The electron density will still satisfy the Boltzmann relation

$$n_e = \lambda A' e^{\tau\psi} \,.$$

The equation of quasi-neutrality in the divertor chamber

$$\Gamma_w P \sqrt{\frac{M}{2T_i}} \int_{\psi_m}^{\psi} d\psi'\, \frac{h(\psi')}{\sqrt{\psi' - \psi}} = n_e - n_H$$

can be solved as before by Abel inversion to give

$$P\left(e^{-\psi_m} - \frac{e^{-\gamma_d\psi_m}}{\gamma_d}\right)h(\eta) = \frac{1}{A'\sqrt{\pi}} \frac{d}{d\eta} \int_0^{\eta} d\eta'\, \frac{n_e(\eta') - n_H(\eta')}{\sqrt{\eta - \eta'}}$$

$$= \frac{d}{d\eta}\left[\frac{2\lambda}{\sqrt{\pi\tau}} e^{\tau\psi_m} e^{-\tau\eta} D(\sqrt{\tau\eta}) - e^{-\psi_m} e^{\eta} \mathrm{erf}(\sqrt{\eta}) - e^{-\psi_m}\right.$$

$$\left. \times (e^{\eta} - 1) + \frac{e^{-\gamma_d\psi_m}}{\gamma_d} \mathrm{erf}(\sqrt{\gamma_d\eta}) + \frac{e^{-\gamma_d\psi_m}}{\gamma_d} (e^{\gamma_d\eta} - 1)\right] . \qquad (48)$$

Now a fraction f_x of the cold ions must appear in region II, so the ionization distribution function can be integrated out to give

$$P\left(e^{-\psi_n} - \frac{e^{-\gamma_d\psi_m}}{\gamma_d}\right)f_x = \frac{2\lambda}{\sqrt{\pi\tau}}\, e^{\tau\psi_d}\, D\left(\sqrt{\tau(\psi_m - \psi)}\right) - e^{\psi_d}\, \mathrm{erf}\left(\sqrt{\psi_m - \psi_d}\right) - e^{-\psi_d} \tag{49}$$

$$+ e^{-\psi_m} + \frac{e^{-\gamma_d\psi_d}}{\gamma_d}\, \mathrm{erf}\left(\sqrt{\gamma_d(\psi_m - \psi_d)}\right) + \frac{e^{-\gamma_d\psi_d}}{\gamma_d} - \frac{e^{-\gamma_d\psi_m}}{\gamma_d}$$

for $$\gamma_d = \frac{e(\phi_d - \phi_t)}{T_i} ,$$

where ϕ_d is the potential just downstream of the constriction in the magnetic field. This is one transcendental equation of ψ_d and ψ_m.

A second equation relating ψ_d and ψ_m is obtained by requiring quasi-neutrality in the throat of the divertor. The hot ion density in the divertor throat is

$$n_{Ht} = 2\pi A e^{-e\phi_t/T_i} \left(\frac{2T_i}{M}\right)^{3/2} \int_{-\infty}^{0} du_\parallel\, e^{-u_\parallel^2} \int_0^\infty du_\perp\, u_\perp e^{-u_\perp^2}$$

$$+ \int_0^{\sqrt{\psi_m}} du_\parallel\, e^{-u_\parallel^2} \int_0^{\sqrt{\gamma_d(\psi_m - u_\parallel^2)}} du_\perp\, u_\perp\, e^{-u_\perp^2}$$

$$= A'\left[1 + \mathrm{erf}\left(\sqrt{\psi_m}\right) - \frac{2\sqrt{R_d - 1}}{\sqrt{\pi}}\, e^{-\gamma_d}\, D\left(\sqrt{(\gamma_d - 1)\psi_m}\right)\right] . \tag{50}$$

The equation for quasi-neutrality in the divertor throat is

$$\frac{A'PR_d}{\sqrt{\pi}} \left(e^{-\psi_m} - \frac{e^{-\gamma_d\psi_m}}{\gamma_d}\right) \int_0^{\psi_m} d\eta' \, \frac{h(\eta')}{\sqrt{\psi_m - \eta'}} = \lambda A' - n_{Ht} .$$

Now $h(\eta)$ is zero for $\eta > \psi_m - \psi_d$ and is given by Eq. (48) for $\eta < \psi_m - \psi_d$,

$$h(\eta) = \left[\frac{d}{d\eta}\int_o^\eta d\eta' \frac{n_e(\eta') - n_H(\eta')}{\sqrt{\eta - \eta'}}\right]\left[A'\sqrt{\pi}\left(e^{-\psi_m} - \frac{e^{-\gamma_d\psi_m}}{\gamma_d}\right)\right]^{-1} .$$

Thus $$\frac{R_d}{\pi}\int_o^{\psi_m-\psi_d} d\eta \frac{1}{\sqrt{\psi_m - \eta}}\frac{d}{d\eta}\int_o^\eta d\eta' \frac{n_e(\eta') - n_H(\eta')}{\sqrt{\eta - \eta'}} = \lambda A' - n_{Ht} ,$$

or $$R_d\int_o^{\psi_m-\psi_d} d\eta' \left[n_e(\eta') - n_H(\eta')\right]\left[\frac{1}{\sqrt{\psi_m - \psi_d - \eta'}} - \frac{\sqrt{\psi_m - \psi_d - \eta'}}{\psi_d}\right] \qquad (51)$$

$$= \pi\sqrt{\psi_d}\left(\lambda A' - n_{Ht}\right) .$$

The integral in Eq. (51) cannot be solved in terms of well-known functions. Numerical integration or further approximations are needed for a solution. This is the second equation for ψ_d and ψ_m which must be solved simultaneously with Eq. (49).

In practice, at typical bundle divertor mirror ratios, there is little difference between the potential at the peak, ψ_m, and the potential immediately downstream of the magnetic constriction, ψ_d; most of the potential variation is in the region in which the magnetic field varies. It is a reasonable approximation then to assume that all cold ions in the divertor throat have essentially the same velocity, that due to the energy of the potential drop where the magnetic field changes. This reduces the problem to a single equation with a single unknown. In this approximation, the equation for quasi-neutrality in the divertor throat is

$$\frac{R_d P f_x}{\sqrt{\pi\psi_m}}\left(e^{-\psi_m} - \frac{e^{-\gamma_d\psi_m}}{\gamma_d}\right) = \lambda - 1 - \mathrm{erf}\left(\sqrt{\psi_m}\right) + \frac{2\sqrt{R_d - 1}}{\sqrt{\pi}} e^{-\gamma_d\psi_m} D\left(\sqrt{(\gamma_d - 1)\psi_m}\right) \qquad (52)$$

which can be solved for ψ_m.

In order to have a potential which has no wells, it is necessary that the potential at the point immediately upstream of the magnetic constriction not have a potential higher than that in the throat. The minimum value of λ for which $\psi_u \leq 0$ can be determined by solving for quasi-neutrality at the upstream point. If ψ_m is small, as is usually the case, then when $\psi_u = 0$, the hot ion density at the upstream point will be

$$n_{Hu} \approx A' \int_{-\infty}^{0} du_{\parallel}\, e^{-u_{\parallel}^2} \int_{0}^{\sqrt{u_{\parallel}^2/(R_u-1)}} du_{\perp}\, u_{\perp} e^{-u_{\perp}^2} = A'\left(1 + \frac{1}{\sqrt{\gamma_u}}\right) ,$$

and the cold ion density is just that in the throat divided by the magnetic field expansion, i.e.,

$$n_c \approx A'\left(\frac{\lambda - 1}{R_u}\right) .$$

So the equation for quasi-neutrality at the upstream point is

$$\lambda = 1 + \frac{1}{\sqrt{\gamma_u}} + \frac{\lambda - 1}{R_u} ,$$

or, using Eq. (30),

$$\lambda = 1 + \sqrt{\gamma_u} . \tag{53}$$

The potential in region I would be computed similarly to the case for a purely falling potential, only here

$$n_H(\psi) = A'\left\{e^{-\psi}\left[1 - \mathrm{erf}\left(\sqrt{\psi_m - \psi}\right)\right] - \frac{e^{-\gamma_d \psi}}{\sqrt{\gamma_d}}\left[1 - \mathrm{erf}\left(\sqrt{\gamma_d(\psi_m - \psi)}\right)\right]\right\} . \tag{54}$$

Solving as before, the equation for quasi-neutrality will be

$$P\left(e^{-\psi_m} - \frac{e^{-\gamma_d\psi_m}}{\gamma_d}\right)h(\eta) = \frac{d}{d\eta}\left[\frac{2\lambda}{\sqrt{\pi\tau}}\, e^{\tau\psi_m} e^{-\tau\eta}\, D\left(\sqrt{\tau\eta}\right) - e^{-\psi_m} e^{\eta} \operatorname{erf}\left(\sqrt{\eta}\right) + e^{-\psi_m}\left(e^{\eta} - 1\right)\right.$$

$$\left. + \frac{e^{-\gamma_d\psi_m}\, e^{\gamma_d\eta}}{\gamma_d} \operatorname{erf}\left(\sqrt{\gamma_d\eta}\right) - \frac{e^{-\gamma_d\psi_m}}{\gamma_d}\left(e^{\gamma_d\eta} - 1\right)\right] .$$

In this case a fraction $(1 - f_x)$ of the neutrals will ionize in region I, hence integrating out $h(\eta)$ gives

$$P\left(e^{-\psi_m} - \frac{e^{-\gamma_d\psi_m}}{\gamma_d}\right)(1 - f_x) = \frac{2\lambda}{\sqrt{\pi\tau}}\, e^{\tau\psi_s}\, D\left(\sqrt{\tau(\psi_m - \psi_s)}\right) - e^{-\psi_s} \operatorname{erf}\left(\sqrt{\psi_m - \psi_s}\right)$$

$$+ e^{-\psi_s} - e^{-\psi_m} + \frac{e^{-\gamma_d\psi_s}}{\gamma_d} \operatorname{erf}\left(\sqrt{\gamma_d(\psi_m - \psi_s)}\right) - \frac{e^{-\gamma_d\psi_s}}{\gamma_d} + \frac{e^{-\gamma_d\psi_m}}{\gamma_d} . \tag{55}$$

The minimum value of λ for monotonicity in region I will be

$$\lambda = \left[e^{-\psi_s} \operatorname{erf}\left(\sqrt{\psi_m - \psi_s}\right) + \frac{e^{-\psi_m}}{\sqrt{\pi(\psi_m - \psi_s)}} - e^{-\psi_s} - e^{-\gamma_d\psi_s} \operatorname{erf}\left(\sqrt{\gamma_d(\psi_m - \psi_s)}\right)\right.$$

$$\left. - \frac{e^{-\gamma_d\psi_m}}{\sqrt{\pi\gamma_d(\psi_m - \psi_s)}} + e^{-\gamma_d\psi_s}\right]\left[\frac{e^{\tau\psi_m}}{\sqrt{\pi(\psi_m - \psi_s)}} - 2\sqrt{\frac{\tau}{\pi}}\, e^{\tau\psi_s}\, D\left(\sqrt{\tau(\psi_m - \psi_s)}\right)\right]^{-1} . \tag{56}$$

Requiring the minimum possible value of λ for monotonicity in both regions I and II will fix the value of f_x. In practice, this choice seems to maximize the energy flow to the divertor.

4. CHARGE EXCHANGE

Thus far, the formation of cold ions in the divertor chamber has implicitly been assumed to be due to electron impact ionization. Actually, at

typical divertor temperatures, charge exchange will be the dominant process in the formation of cold ions [8]. The main effect of ionization and charge exchange is the same: the production of cold ions. Only the distinctions between charge exchange and ionization have been ignored. Explicitly distinguishing charge exchange from ionization produces three effects:

(1) The hot ion density in the divertor will be lower since charge exchange will replace hot ions with cold ions.

(2) The cold ion density will increase, since charge exchange will replace cold ions which have acquired a velocity by falling through a potential gradient with slower cold ions, and the same flux at a slower velocity implies an increased density.

(3) The total ion flux to the divertor will increase, since ions that have been treated as reflecting off the potential peak may charge exchange before leaving the divertor. In an enclosed chamber, hot neutrals hitting the side walls will also contribute to the neutral density.

The production of cold ions by charge exchange is already included in the cold ion source in Section 2. The other effects of charge exchange are small enough to treat them as a perturbation. The potential and density profiles in the divertor can be initially computed neglecting charge exchange; charge exchange effects are then computed using these profiles, new potential and density profiles computed, and the system iterated until it converges.

Let n_o be the density of neutral gas in the divertor. The net source rate of cold ions will be

$$S_C = n_o n_e \langle \sigma v_e \rangle_i + n_o n_H \langle \sigma v_H \rangle_{cx} \, . \tag{57}$$

Here the first term represents the production of cold ions due to electron impact ionization of neutrals and the second term represents production due to charge exchange of hot ions with neutrals. Since charge exchange of neutrals with cold ions does not alter the number of cold ions, only their average velocity, this reaction does not appear in Eq. (57). Therefore,

$$n_o = \frac{S_C}{n_e \langle \sigma v_e \rangle_i + n_H \langle \sigma v_H \rangle_{cx}} .$$

The decrease in the flux of hot ions due to charge exchange will be

$$\frac{d\Gamma_H}{dx} = \int d^3 v_H \; f(x, v_H) \; \sigma_{cx} v_H n_o(x) ,$$

where $f(x,v_H)$ is the hot ion distribution function. In terms of η,

$$\frac{d\Gamma_H}{d\eta} = \int d^3 v_H \; f(\eta, v_H) \; \sigma_{cx} \frac{S_C(\eta)}{n_e(\eta) \langle \sigma v_e \rangle_i + n_H(\eta) \langle \sigma_{cx} v_H \rangle} ,$$

where

$$S_C(\eta) = S_C(x(\eta)) \frac{dx}{d\eta} .$$

The relationship between the source function $S_C(\eta)$ and the normalized source function $h(\eta)$ is

$$S_C(\eta) = \Gamma_w P h(\eta) ,$$

so

$$\frac{d\Gamma_H}{d\eta} = \int d^3 v_H \; f(\eta, v_H) \langle \sigma_{cx} v_H \rangle \frac{\Gamma_w P h(\eta)}{n_e \langle \sigma v_e \rangle_i + n_H \langle \sigma_{cx} v_H \rangle} .$$

In region II it is convenient at this point to divide the ion flux into the

downstream-going ions and the reflected, upstream-going ions. Averaging over the velocities gives

$$\Gamma_+(\eta) - \Gamma_+^o(\eta) = -\int_{\eta}^{\psi_m-\psi_d} d\eta' \frac{n_H^+(\eta')\langle\sigma v_H\rangle_{cx}\Gamma_w Ph(\eta)}{n_e(\eta')\langle\sigma v_e\rangle_i + n_H^+(\eta')\langle\sigma v_H\rangle_{cx}},$$

where Γ_+^o is the downstream-going ion flux in the absence of charge exchange effects and n_H^+ is the downstream-going hot ion density. For a uniform magnetic field, $\psi_d = 0$. If the approximation is made that the hot ion density is diminished to the same extent as is the flux, then

$$\frac{\Gamma_+(\eta)}{\Gamma_+^o(\eta)} = \frac{n_H^+(\eta)}{n_H^{+o}(\eta)} = 1 - \int_{\eta}^{\psi_m-\psi_d} d\eta' \frac{n_H^+(\eta')\langle\sigma v_H\rangle_{cx}\Gamma_w Ph(\eta')}{\Gamma_+^o(\eta)\left[n_c(\eta')\langle\sigma v_e\rangle_i + n_H^+(\eta')\langle\sigma v_H\rangle_{cx}\right]}. \quad (58)$$

For particles that reflect off of the rising potential, it is necessary to integrate to the particle turning point and back, thus

$$\frac{n_H^-(\eta)}{n_H^{o-}(\eta)} = 1 - \int_{\eta_{turn}}^{\psi_m-\psi_d} d\eta' \frac{n_H^-(\eta')\langle\sigma v_H\rangle_{cx}\Gamma_w Ph(\eta')}{\Gamma_-^o(\eta)\left[n_e(\eta')\langle\sigma v_e\rangle_i + n_H^+(\eta')\langle\sigma v_H\rangle_{cx}\right]}. \quad (59)$$

where n_H^- is the reflected hot ion density, n_H^o and Γ_-^o are the reflected density and particle flux in the absence of charge exchange corrections, and η_{turn} is some average turning point. A reasonable approximation is that $\eta_{turn} = 1/2\ \eta$, i.e. the average reflected particle turns halfway between the observation point and the potential peak.

In region I (beyond the peak in the potential) there will be no reflected ions. The diminution in the downstream-going flux can be computed as

$$\frac{\Gamma_+(\eta)}{\Gamma_+^o(\eta)} = \frac{n_H^+(\eta)}{n_H^{+o}(\eta)} = \frac{\Gamma_+(\eta=0)}{\Gamma_o^+(\eta=0)} - \int_o^{\eta} \frac{n_H^+(\eta')\langle\sigma v_H\rangle_{cx}\Gamma_w Ph(\eta')}{\Gamma_+^o(\eta)\left[n_e(\eta')\langle\sigma v_e\rangle_i + n_H\langle\sigma v_H\rangle_{cx}\right]}. \quad (60)$$

where the first term on the right hand side is the fractional charge exchange loss in region II; i.e. $\eta = 0$ at the potential peak.

The hot ion flux to the wall when charge exchange effects are included is

$$\Gamma_w = \Gamma_H(\eta=\psi_m-\psi_d) - \Gamma_-^o(\eta=\psi_m-\psi_d)\,\frac{n_H(\eta=\psi_m-\psi_d)}{n_H^o(\eta=\psi_m-\psi_d)}\,, \tag{61}$$

that is, the flux entering the divertor minus the reflected portion that does not undergo charge exchange.

Charge exchange of cold ions substitutes a slower cold ion for a faster cold ion and so increases the density of cold ions without directly affecting the cold ion flux. The increased density due to cold ion charge exchange will be the charge exchange rate times the difference in the inverses of the cold ion velocity due to the charge exchange. That is

$$\begin{aligned} n_{cor}(\eta) = \Gamma_w P \sqrt{\frac{M}{2T_i}} \int_o^\eta d\eta' \,\frac{h(\eta')}{\sqrt{\eta-\eta'}}\,\frac{\sigma_{cx}}{n_e(\eta')\langle\sigma v_e\rangle_i + n_H\langle\sigma v_H\rangle_{cx}} \\ \times\, \Gamma_w P \int_o^{\eta'} d\eta''\, h(\eta'')\left(\frac{1}{\sqrt{\eta-\eta'}} - \frac{1}{\sqrt{\eta-\eta''}}\right)\,. \end{aligned} \tag{62}$$

Then Eq. (45) becomes

$$\Gamma_w P \sqrt{\frac{M}{2T_i}} \int_o^\eta d\eta' \,\frac{h(\eta')}{\sqrt{\eta-\eta'}} = n_e(\eta) - n_H(\eta) - n_{cor}(\eta)\,. \tag{63}$$

The value of n_{cor} can be computed using the source profiles from the previous iteration. The solution can be iterated until the values of $h(\eta)$ converge.

The above technique used to account for charge exchange effects is quite approximate and cannot be expected to give results of high accuracy. Error

has also been introduced from the neglect of reionization of charge exchange neutrals and the assumption of a single value of the charge exchange cross-section, independent of the specific ion energy. It turns out, however, that the effects of charge exchange are usually fairly small. Thus, highly accurate procedures are not required.

5. RESULTS AND DISCUSSION

The model developed in the previous sections has been used to calculate the potentials and particle densities for a variety of divertor configurations and plasma parameters. In addition, the power carried by ions and electrons entering the divertor chamber, the power carried by ions and electrons incident on the divertor target, the power carried by neutrals hitting the divertor walls, and the power carried by cold ions going from the divertor chamber to the scrape-off layer in the torus have all been evaluated.

Table I shows a number of input and output parameters from ten representative sets of divertor configurations and plasma parameters. Table II explains the meanings of the listed parameters. The absolute magnitude of the ion and electron temperatures do not explicitly enter the calculations. They only affect the calculations through the ratio of the charge exchange cross-section to electron impact ionization cross-section σ_{cx}/σ_i. Half of the cases have $\tau = 1$ and $\sigma_{cx}/\sigma_i = 50$, values appropriate for $T_i = T_e = 100$ eV [8]. Several other cases are treated as well. In all the cases the values of f_x and λ are chosen so as to give the maximum energy unload for the given values of R_u, R_d, f_p, τ, and σ_{cx}/σ_i. Case 1 (Fig. 7) depicts the case of the minimum pumping ($f_p = 0.6$) which gives a potential which falls monotonically from the

TABLE I. PARAMETERS FOR A VARIETY OF REPRESENTATIVE DIVERTOR AND PLASMA CONFIGURATIONS

Case	R_u, R_d	f_p	τ	σ_{cx}/σ_i	λ	f_x	ψ_m	ψ_w	ψ_c	Q_e	Q_i	Q_{we}	Q_{wH}	Q_{wC}	Q_{wn}
1	1.0	0.6	1.0	50.	2.0	0.0	0.0	-3.4	0.0	7.8	2.0	2.9	4.2	2.2	0.5
2	1.0	0.0	1.0	50.	2.8	0.35	0.18	-3.3	-0.17	8.6	1.6	2.6	2.2	4.5	0.9
3	2.0	0.36	1.0	50.	2.0	0.0	0.0	-3.6	0.0	7.0	1.0	2.6	2.1	3.1	0.3
4	2.0	0.0	1.0	50.	2.4	0.25	0.18	-3.3	-0.09	8.4	0.8	2.8	1.5	4.6	0.4
5	4.0	0.0	1.0	50.	2.1	0.14	0.27	-3.3	-0.4	8.5	0.4	3.0	0.8	5.0	0.2
6	1.0	0.0	1.0	0.	2.6	0.35	0.22	-3.2	-0.14	9.7	1.4	2.6	3.6	3.5	0.0
7	1.0	1.0	1.0	270.	3.6	0.37	0.11	-3.6	-0.29	7.1	1.4	1.8	1.1	4.3	1.4
8	2.0	2.0	1.0	0.	2.4	0.24	0.20	-3.3	-0.09	7.9	0.8	2.7	2.3	3.7	0.0
9	1.0	0.0	3.0	67.	3.4	0.41	0.10	-1.0	-0.13	2.5	1.7	0.7	1.2	1.3	1.1
10	2.0	0.0	3.0	67.	2.4	0.28	0.18	-1.0	-0.05	2.6	0.9	0.9	0.8	1.3	0.4

R_u, R_d Ratio of the magnetic field strength in the divertor throat to that in the scrape-off layer and divertor chamber.

f_p Fraction of the ions and hot neutrals striking the wall that are pumped away before recycling.

τ Ratio of the hot ion temperature to the electron temperature.

$\frac{\sigma_{cx}}{\sigma_i}$ Ratio of the charge exchange cross section to the electron impact ionization cross section.

λ Normalized electron density in the divertor throat. If the ion density is a half-sided Maxwellian, then $\lambda = 1.0$.

f_x Fraction of the cold ions created which are born in region II and so flow back towards the scrape-off layer.

ψ_m Normalized maximum potential in the divertor chamber, relative to the divertor throat, $e(\phi_m - \phi_t)/T_i$.

ψ_w Normalized potential at the wall, relative to the divertor throat, $e(\phi_w - \phi_t)/T_i$.

ψ_c Normalized potential in the scrape-off layer relative to the divertor throat, i.e. $e(\phi_c - \phi_t)/T_i$.

Q_e Net energy flux from the electrons in the scrape-off layer.

Q_i Net energy flux from the ions in the scrape-off layer.

Q_{we} Energy flux to the wall from the electrons.

Q_{wH} Energy flux to the wall from hot ions.

Q_{wC} Energy flux to the wall from cold ions.

Q_{wn} Energy flux to the wall from neutrals.

The energy fluxes, Q_e, Q_i, Q_{we}, Q_{wH}, Q_{wC}, Q_{wn}, are normalized to $n_i T_i \sqrt{T_i/M}$, where n_i is the ion density in the scrape-off layer.

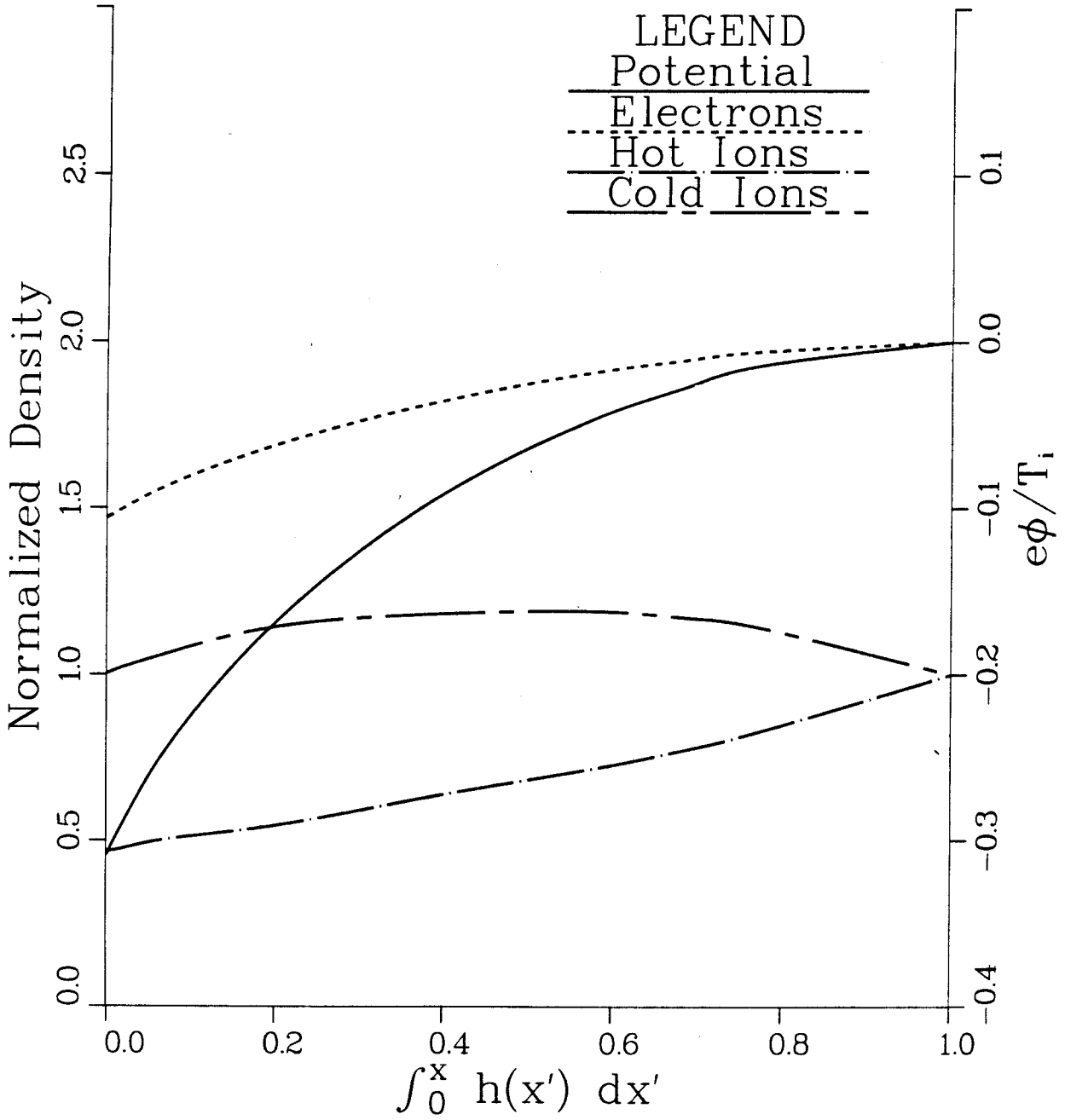

Fig. 7. Electric potential and density profiles for the case with the minimum pumping for an electric potential that falls monotonically from the scrape-off layer to the divertor target in a divertor with a uniform magnetic field. Potentials are shown relative to the scrape-off layer potential. $T_e = T_i = 100$ eV, $\lambda = 2.0$.

scrape-off layer to the target plate in a uniform magnetic field. Case 2 (Fig. 8) depicts the same situation with no pumping.

Case 3 and case 4 (Fig. 9) portray a bundle divertor with a mirror ratio equal to 2, with different amounts of pumping. A monotonically falling potential is possible with less pumping (39%) with a bundle divertor than is required with a uniform magnetic field (60%). This is because the downstream expansion in the magnetic field reduces the ion density and contributes to the falling potential.

Case 5 treats the case of a bundle divertor with a mirror ratio of 4. If there were no electric field and no refluxing ions, the hot ion energy flux, Q_i, would equal $2/R_u$; e.g. if the upstream mirror ratio were 2, about half of the ions encountering the magnetic constriction in the divertor throat would be reflected, and about half would enter the divertor. The electric field and the refluxing of cold ions does not alter this enormously.

The electron energy flux is not strongly dependent on the mirror ratio since at lower ion fluxes the electric potential drop from the scrape-off layer to the wall is greater; i.e. electrons must be more strongly repelled in order to give ambipolar flow to the wall; and so the energy per particle striking the wall is greater. Cold ions will be accelerated to the wall as well.

Cases 6-8 depict situations with different amounts of charge exchange. Charge exchange converts hot ions into hot neutrals which reduces the ion current to the wall, and so the wall sheath potential drop increases. Very large amounts of charge exchange, as in case 7, are not well handled with the low order charge exchange corrections that are included in the divertor model. Still, the qualitative effects of charge exchange should be correct.

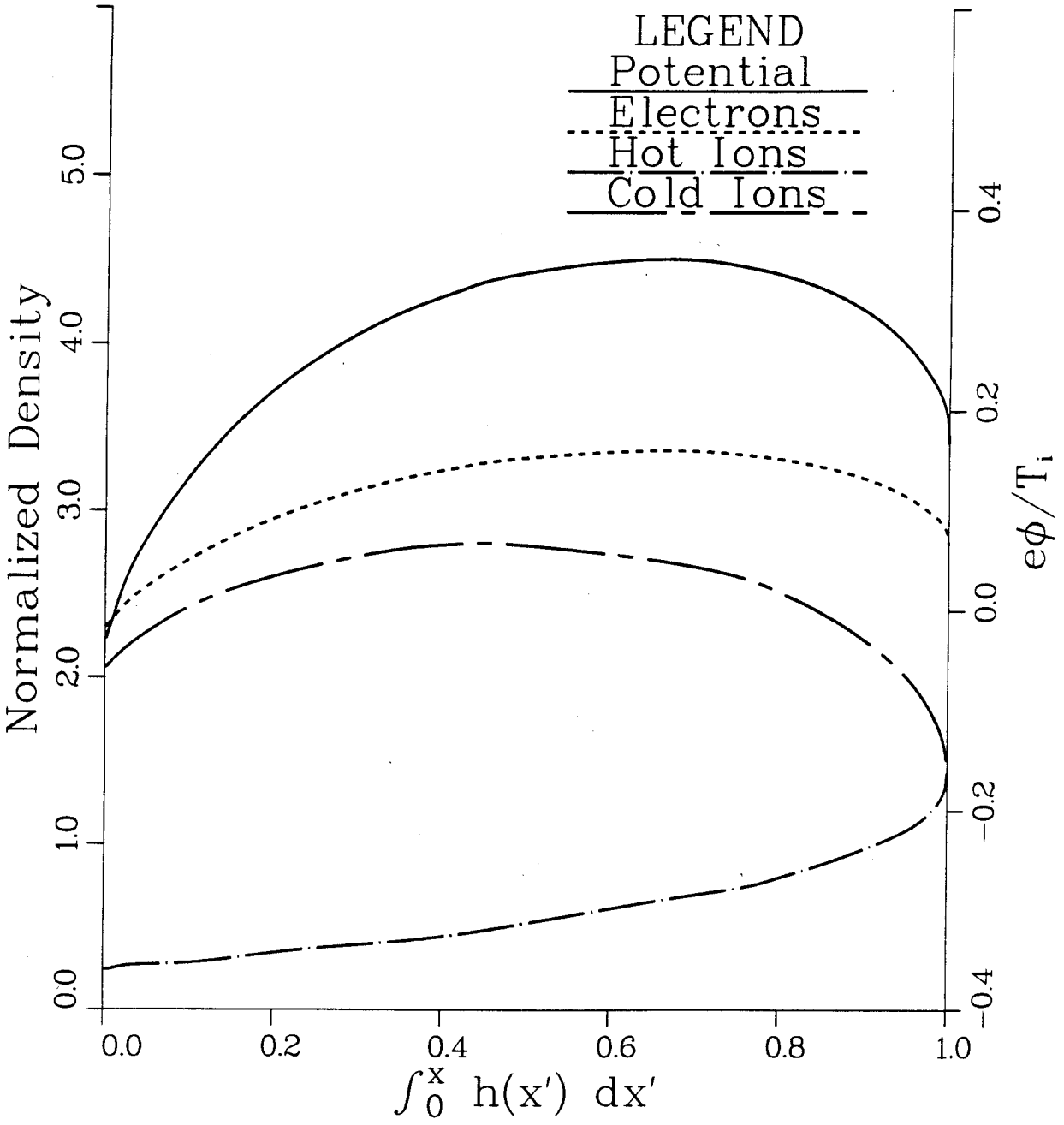

Fig. 8. Electric potential and density profiles for the case of a divertor with no pumping and a uniform magnetic field. Potentials are shown relative to the scrape-off layer potential. $T_e = T_i = 100$ eV, $\lambda = 2.8$.

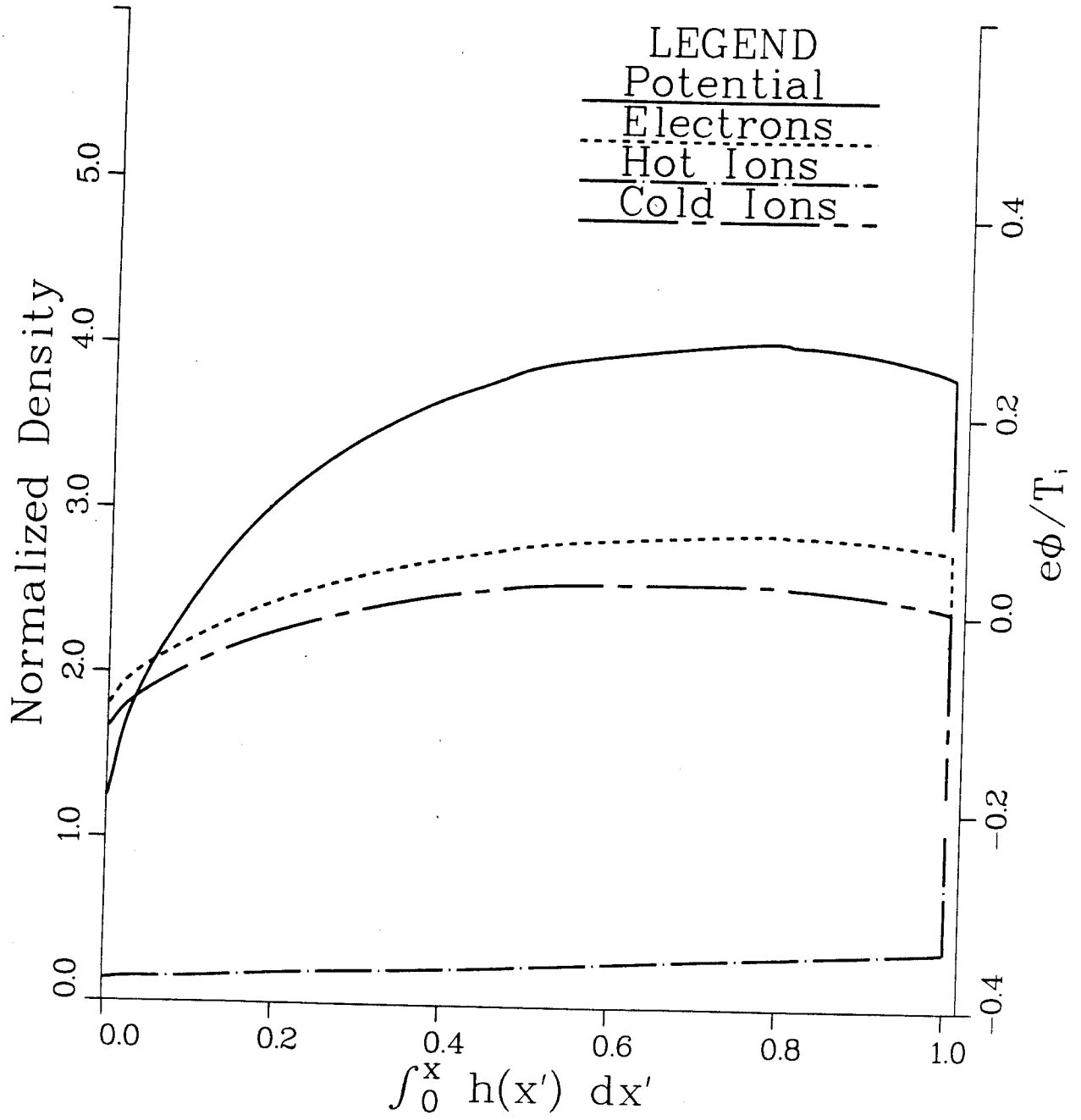

Fig. 9. Electric potential and density profiles for the case of a divertor with no pumping and $R_u = R_d = 2.0$. Potentials are shown relative to the scrape-off layer potential. $T_e = T_i = 100$ eV, $\lambda = 2.4$.

In cases 9 and 10 the hot ion temperature is three times greater than the electron temperature. Ions are frequently hotter than electrons in the scrape-off layer of tokamaks. Compared to hotter electrons, cooler electrons require less of a potential difference to produce the same change in the electron density.

The electron energy flow to the wall is the value for a Maxwellian electron distribution where the wall potential is set by requiring ambipolar flow to the wall. Secondary electron emission is ignored. The ion energy flows are computed by taking the energy moments of the ion distributions. The electron energy flux from the scrape-off layer is set equal to the difference in the total energy flux to the wall and the net ion energy flux from the scrape-off layer. Details are given in Appendix A.

In most cases, while the energy flow to the plate is primarily due to ions, the energy loss from the scrape-off layer is mostly electron energy. This is because the electrons are responsible for maintaining the electric potential that accelerates the ions into the plate. When the electron temperature is considerably lower than the ion temperature (cases 9 and 10), the ion energy loss is a more significant fraction of the total energy loss from the scrape-off zone.

The results presented here are in substantial agreement with the numerical simulations by Gierzewski et al. [1], except for the fact that here the effects of charge exchange are more pronounced. The discrepancy may be due to the fact that here all hot ions that charge exchange are assumed to strike the divertor end or side walls as hot neutrals, while they follow these charge exchange neutrals and allow them to reionize or escape the divertor. The treatment here is more suitable for a constricted divertor channel while that of

Gierzewski et al. is more suitable for a more open situation such as is found with a limiter.

In their kinetic simulations of plasma flow to a limiter in a uniform magnetic field, Gierzewski et al. also find a minimum value for the cold ion density in the divertor. For the case with no pumping and $T_e = T_i = 1$ keV, they find the minimum value of the ratio of the cold H_2^+ ion density to the hot H^+ ion density at the potential peak to be equal to approximately 3.6 [9]. The model presented here neglects the initial formation of H_2^+ ion and treats only the fully ionized H^+ ions. Here the ratio of the cold ion density to the hot ion density is 8.1 where $\sigma_{cx}/\sigma_i = 270$, as is appropriate at this temperature (case 7). A better match is obtained with $\sigma_{cx}/\sigma_i = 50$ (case 2), the ratio being 3.4. Lower cross section ratios also give better agreement in the value of the peak electric potential. Gierzewski et al. find $\psi_m \approx 0.18$. Here the values are $\psi_m = 0.11$ for $\sigma_{cx}/\sigma_i = 270$ and $\psi_m = 0.18$ for $\sigma_{cx}/\sigma_i = 50$. The effect of reionization of charge exchange neutrals can be introduced qualitatively by reducing the ratio σ_{cx}/σ_i; this would bring our results into closer agreement with those of Gierzewski et al.

The original simulation of Gierzewski et al. only carried the computations up to the potential peak. Computations have now been performed which carry the simulation beyond the peak and through the plasma sheath [10]. These simulations indicate that only a small fraction of the cold ions produced will reflux to the wall, while here it is found that profiles are possible in which the majority of cold ions reflux to the wall and that these profiles give the maximum energy unload. The discrepancy has not yet been resolved. The amount of recycling in the divertor chamber is important in that it alters the energy flux to the target plate. If the region of electric

field pointing towards the plate is large enough, then sputtered wall material will be ionized in this region and returned to the plate rather than entering the main plasma. Morse et al. [10] have not yet extended their simulations from the divertor throat back into the scrape-off layer. Thus, there is as yet no check on the accuracy of the simple estimate (25) used here for the potential difference between the scrape-off layer and the divertor throat.

The results presented here are also in qualitative agreement with the fluid simulations of Petravic et al. [2]. They find that in weakly pumped divertors there is a large increase in the density near the target plate. A similar density rise is also predicted here, as well as in the simulations of Gierzewski et al.

APPENDIX A. ENERGY FLOW

The energy flow to the divertor can be calculated from an energy balance:

Energy from the scrape-off layer = Energy to the divertor walls

or in more detail

Electron energy from the scrape-off layer + Hot ion energy from the scrape-off layer - Energy to the scrape-off layer from cold ions = Electron energy to the divertor target + Hot ion energy to the divertor target + Cold ion energy to the divertor target + Hot neutral energy to the divertor walls + Cold neutral energy to the divertor walls .

All of these except the electron energy from the scrape-off layer can be calculated explicitly. That final quantity can be determined from the energy balance. All the following assumes that the electrons are responsible for maintaining the potential profiles and the energy which ions acquire from falling through a potential difference ultimately comes from the electrons.

For a potential that falls monotonically from the scrape-off layer to the divertor target, the hot ion energy loss from the scrape-off layer will be

$$Q_H = 4\tilde{A} \int_0^\infty du_\parallel \, u_\parallel e^{-u_\parallel^2} \int_0^{\sqrt{(u_\parallel^2+\psi_c)/(R_u-1)}} du_\perp \, u_\perp e^{-u_\perp^2} (u_\parallel^2 + u_\perp^2)$$

$$= \tilde{A}\left[2 - \frac{(1 - \gamma_u)(R_u - 1)(1 + \gamma_u\psi_c)}{\gamma_u^2(R_u - 1)} e^{-\psi_c/(R_u-1)}\right. \tag{A.1}$$

where

$$\tilde{A} = \frac{2\pi T_i^3 R_d}{M^2 R_u} e^{-\psi_c} A \ . \tag{A.2}$$

The factor R_d/R_u accounts for the change in the area of a flux tube in a bundle divertor. A uniform beam of cold ions with velocity

$$v = \sqrt{\frac{2T_i}{M}} \tag{A.3}$$

would have an energy flux per unit area of $\tilde{A}$.

For a peaked potential, there is the requirement that

$$\begin{aligned} \psi_c + u_{\parallel c}^2 + u_{\perp c}^2 &= u_{\parallel t}^2 + u_{\perp t}^2 \\ &\geq u_{\perp t}^2 \\ &\geq R_u u_{\perp c}^2 \end{aligned} \tag{A.4}$$

or

$$u_\perp^2 \leq \frac{u_{\parallel c}^2 + \psi_c}{R_u - 1} \tag{A.5}$$

and also the requirement that

$$\begin{aligned} \psi_c + u_{\parallel c}^2 + u_{\perp c}^2 &= u_{\parallel m}^2 + u_{\perp m}^2 + \psi_m \\ &\geq u_{\perp m}^2 + \psi_m \\ &\geq (R_u/R_d)\ u_{\perp m}^2 + \psi_m \ . \end{aligned} \tag{A.6}$$

These conditions intersect when

$$u_{\parallel c}^2 = \frac{\gamma_d}{\gamma_u} \psi_m - \psi_c \ . \tag{A.7}$$

If $R_u > R_d$, the hot ion energy loss from the scrape-off layer will be

$$Q_H = 4\tilde{A}\Big[\int_{\sqrt{\psi_m-\psi_c}}^{\sqrt{(\gamma_d/\gamma_u)\psi_m-\psi_c}} du_\parallel\, u_\parallel e^{-u_\parallel^2} \int_0^{\sqrt{(u_\parallel^2+\psi_c-\psi_m)/((R_u/R_d)-1)}} du_\perp\, u_\perp e^{-u_\perp^2(u_\parallel^2+u_\perp^2)}$$

$$+ \int_{\sqrt{(\gamma_d/\gamma_u)\psi_m-\psi_c}}^{\infty} du_\parallel\, u_\parallel e^{-u_\parallel^2} \int_0^{\sqrt{(u_\parallel^2+\psi_c)/(R_u-1)}} du_\perp\, u_\perp e^{-u_\perp^2(u_\parallel^2+u_\perp^2)}\Big] , \tag{A.8}$$

and in the case where $R_u < R_d$ it will be

$$Q_H = 4\tilde{A}\Big[\int_{\sqrt{(\gamma_d/\gamma_u)\psi_m-\psi_c}}^{\sqrt{\psi_m-\psi_c}} du_\parallel\, u_\parallel e^{-u_\parallel^2} \int_{\sqrt{(\psi_m-\psi_c-u_\parallel^2)/(1-(R_d/R_u))}}^{\sqrt{(u_\parallel^2+\psi_c)/(R_u-1)}} du_\perp\, u_\perp e^{-u_\perp^2(u_\parallel^2+u_\perp^2)}$$

$$+ \int_{\sqrt{\psi_m-\psi_c}}^{\infty} du_\parallel\, u_\parallel e^{-u_\parallel^2} \int_0^{\sqrt{(u_\parallel^2+\psi_c/(R_u-1)}} du_\perp\, u_\perp e^{-u_\perp^2(u_\parallel^2+u_\perp^2)}\Big] . \tag{A.9}$$

Both expressions can be integrated to give

$$Q_H = \tilde{A}\{e^{\psi_c}(2 - \psi_m - \psi_c)e^{-\psi_m} - \frac{e^{(R_d\psi_m)/(R_u-R_d)}}{|\gamma_h|}\left[(2 + \psi_m - \psi_c)e^{-\gamma_h\psi_m}\right.$$

$$\left. - (2 - \gamma_d\psi_m - \psi_c)e^{-\gamma_h(\gamma_d/\gamma_u)\psi_m}\right] - \left(\frac{2 + \gamma_d\psi_m - \psi_c}{\gamma_u}\right) e^{-\gamma_d\psi_m}\} . \tag{A.10}$$

Only the first term will be present for a uniform field.

For a monotonically falling potential, the hot ion energy flux to the wall will be, for $R_d < R_u$

$$Q_{wH} = 4\tilde{A}\frac{R_d}{R_u} e^{\psi_c-\psi_w}\Big[\int_{\sqrt{(\gamma_u/\gamma_d)\psi_u-\psi_w}}^{\sqrt{\psi_u-\psi_w}} du_\parallel\, u_\parallel e^{-u_\parallel^2} \int_{\sqrt{\gamma_h(\psi_u-\psi_w-u_\parallel^2)}}^{\sqrt{(u_\parallel^2+\psi_w)/(R_d-1)}} du_\perp\, u_\perp e^{-u_\perp^2}(u_\parallel^2+u_\perp^2)$$

$$+\int_{\sqrt{\psi_u-\psi_w}}^{\infty} du_\parallel\, u_\parallel e^{-u_\parallel^2}\int_0^{\sqrt{(u_\parallel^2+\psi_w)/(R_d-1)}} du_\perp\, u_\perp e^{-u_\perp^2}(u_\parallel^2+u_\perp^2)\Big]$$

$$= \tilde{A}\frac{R_d}{R_u} e^{\psi_c}\{(2+\psi_u-\psi_w)e^{-\psi_u} - e^{\gamma_u\psi_u}\left(\frac{2+\gamma_u\psi_u-\psi_w}{\gamma_d}\right) + e^{-\gamma_h\psi_w}\frac{R_u}{R_d} \qquad (A.11)$$

$$\times(\psi_u-\psi_w)\left[1-(\gamma_h-1)\left(\frac{\gamma_u}{\gamma_d}\psi_u-\psi_w\right)e^{-(\gamma_h-1)(\gamma_u/\gamma_d)\psi_u}\right.$$

$$\left.-\left(1-(\gamma_h-1)(\psi_u-\psi_w)\right)e^{-(\gamma_h-1)\psi_u}\right]\}$$

for
$$\psi_w = \frac{e\phi_w}{T_i}\,. \qquad (A.12)$$

where ϕ_w is the potential on the wall side of the plasma sheath. For the case where $R_u < R_d$ it will be

$$Q_{wH} = 4\tilde{A}\frac{R_d}{R_u} e^{\psi_c-\psi_w}\Big[\int_{\sqrt{\psi_u-\psi_w}}^{\sqrt{(\gamma_u/\gamma_d)\psi_u-\psi_w}} du_\parallel\, e^{-u_\parallel^2}\int_0^{\sqrt{|\gamma_h|(u_\parallel^2+\psi_w-\psi_u)}} du_\perp\, u_\perp e^{-u_\perp^2}(u_\parallel^2+u_\perp^2)$$

$$+\int_{\sqrt{(\gamma_u/\gamma_d)\psi_u-\psi_w}}^{\infty} du_\parallel\, e^{-u_\parallel^2}\int_0^{\sqrt{(u_\parallel^2+\psi_w)/(R_d-1)}} du_\perp\, u_\perp e^{-u_\perp^2}(u_\parallel^2+u_\perp^2)\Big]$$

$$= \tilde{A}\frac{R_d}{R_u}e^{\psi_c}\{(2+\psi_u-\psi_w)e^{-\psi_u} - e^{\gamma_u\psi_u}(\frac{2+\gamma_u\psi_u-\psi_w}{\gamma_d}) + e^{\gamma_h\psi_u}[\frac{2}{1-\gamma_h}$$

$$+\frac{R_u}{R_d}(\psi_u-\psi_w)][(1-(\gamma_u-1)(\frac{\gamma_u}{\gamma_d}\psi_u-\psi_w))e^{-(\gamma_h-1)(\gamma_u/\gamma_d)\psi_u} \qquad (A.13)$$

$$-(1-(\gamma_h-1)(\psi_u-\psi_w))e^{(\gamma_h-1)(\gamma_u/\gamma_d)\psi_u}]\} .$$

For a rising potential the energy flux to the plate will be

$$Q_{wH} = \tilde{A}\frac{R_d}{R_u}e^{\psi_c-\psi_w}\int_{\sqrt{\psi_m-\psi_w}}^{\infty} du_\parallel\, u_\parallel e^{-u_\parallel^2}\int_0^{\sqrt{(u_\parallel^2+\psi_w)/(R_d-1)}} du_\perp\, u_\perp e^{-u_\perp^2}(u_\parallel^2+u_\perp^2)$$

$$= \tilde{A}\frac{R_d}{R_u}e^{\psi_c}(2+\psi_m-\psi_w)e^{-\psi_m} - \frac{e^{-\gamma_d\psi_m}}{\gamma_d}[(\frac{R_d+\gamma_d(\psi_m+R_d-1)}{\gamma_d(R_d-1)}+\psi_m-\psi_w)] . \qquad (A.14)$$

The energy cold ions return to the scrape-off layer will be

$$Q_{sC} = \tilde{A}e^{\psi_c}\frac{R_d}{R_u}\int_0^{\psi_m-\psi_c} d\eta\,\frac{P\Gamma_w h(\eta)}{A'\sqrt{2T_i/\pi M}}(\psi_m-\psi_c-\eta) . \qquad (A.15)$$

Now $h(\eta) = 0$ for $\eta = \psi_m - \psi_d$ and

$$h(\eta) = \frac{A'\sqrt{2T_i/\pi M}}{\sqrt{\pi}\,P\Gamma_w}\frac{d}{d\eta}\int_0^{\eta} d\eta'\,\frac{n_e(\eta')-n_{iH}(\eta')}{\sqrt{\eta-\eta'}} \qquad (A.16)$$

so this will be

$$Q_{sC} = \frac{\tilde{A}}{\sqrt{\pi}}\frac{R_d}{R_u}e^{\psi_c}\int_0^{\psi_m} d\eta\,(\psi_m-\psi_c-\eta)\frac{d}{d\eta}\int_0^{\eta} d\eta'\,\frac{n_e(\eta')-n_{iH}(\eta')}{\sqrt{\eta-\eta'}} . \qquad (A.17)$$

Solving gives

$$Q_{sC} = \frac{\tilde{A}}{\sqrt{\pi}} \frac{R_d}{R_u} e^{\psi_c} \int_o^{\psi_m - \psi_d} d\eta' \left[\frac{\psi_d - \psi_c}{\sqrt{\psi_m - \psi_d - \eta'}} + 2\sqrt{\psi_m - \psi_d - \eta'} \right] \left[n_e(\eta') - n_{iH}(\eta') \right] . \tag{A.18}$$

Similarly, the energy flux from cold ions falling to the wall will be

$$Q_{wC} = \frac{\tilde{A}}{\sqrt{\pi}} \frac{R_d}{R_u} e^{\psi_c} \int_o^{\psi_m - \psi_s} d\eta' \left[\frac{\psi_s - \psi_w}{\sqrt{\psi_m - \psi_s - \eta'}} + 2\sqrt{\psi_m - \psi_s - \eta'} \right] \left[n_e(\eta') - n_{iH}(\eta') \right] . \tag{A.19}$$

These integrals must be solved numerically, or approximations must be made in order to do the integration.

The wall potential ψ_w can be computed by requiring ambipolar particle flow to the wall. This gives

$$\psi_w = \frac{1}{\tau} \ln \left[\frac{2}{\lambda} \frac{\Gamma_w}{A' \sqrt{2T_i/\pi M}} P\sqrt{\pi} \, (1 + C_{se}) \sqrt{\frac{m}{M}} \right] , \tag{A.20}$$

where C_{se} is the secondary electron emission coefficient for the wall material and m is the electron mass.

The electron energy flux to the wall will be

$$Q_{we} = 2 \frac{R_d}{R_u} e^{\psi_c} e^{\psi_w} \sqrt{\frac{M}{m\tau^3}} . \tag{A.21}$$

In all cases in this chapter the effects of charge exchange have been ignored. The hot and cold neutral energy fluxes and the corrections to the

ion and electron energy fluxes are usually fairly small. They can (and have been) numerically included in computations, but are not presented here.

Using all the expressions, the electron energy flux from the scrape-off layer can be computed.

ACKNOWLEDGEMENTS

The authors would like to thank P. McKenty and R. Morse for useful and stimulating discussions. This work was supported by the U.S. Department of Energy.

REFERENCES

[1] GIERZEWSKI, P., MCKENTY, P., MCCULLEN, J., MORSE, R., Phys. Rev. Lett. 49 (1982) 650.

[2] PETRAVIC, M., POST, D., HEIFETZ, D., SCHMIDT, J., Phys. Rev. Lett. 48 (1982) 326.

[3] SEKI, Y., SHIMOMURA, Y., MAKI, K., AZUMI, M., TAKIZUKA, T., Nucl. Fusion 20 (1980) 1213.

[4] PEARSON, C.E., Handbook of Applied Mathematics, Van Nostrand Reinhold, New York, NY (1974) 615.

[5] ABRAMOWITZ, M., STEGUN, I.A., Handbook of Mathematical Functions, Ch. 7, National Bureau of Standards (1972) 319.

[6] BAILEY, A.W., EMMERT, G.A., J. Nucl. Mater. 111/112 (1982) 403.

[7] EMMERT, G.A., University of Wisconsin Fusion Engineering Program Report UWFDM-343 (1980).

[8] FREEMAN, R.L., JONES, E.M., Culham Lab. Rep. CLM-R 137 (1974).

[9] GIERZEWSKI, P., MCKENTY, P., MCCULLEN, J., MORSE, R., University of Arizona, Private Communication (3 October 1981).

[10] MORSE, R., GIERSEWSKI, P., MCCULLEN, J., University of Arizona, Private Communication (21 March 1983).